Electronic Supplementary Information

Table of Contents

1. General

Unless otherwise noted, all starting materials were obtained from commercial suppliers and used without further purification. ^{1}H and ^{13}C NMR spectra were recorded on Bruker NMR spectrometers (400 MHz, or 600 MHz) with TMS as reference. ESI Mass spectra were recorded on an Esquire 6000 spectrometer (LC/MS). Single crystal X-ray diffraction data were collected on a SMART APEX 2 X-ray diffractometer equipped with a normal focus Mo-target X-ray tube (λ = 0.71073 Å. Data reduction included absorption corrections by the multi-scan method. The structures were solved by direct methods and refined by full-matrix least-squares using SHELXS-97. All non-hydrogen atoms were refined anisotropically and hydrogen atoms were added at their geometrically ideal positions and refined isotropically. The DFT-optimized calculation was carried out with B3LYP hybrid exchange-correlation functional and DGTZVP set.[1,2] The PCM model were used to simulate the different solution effect.[3] The ECD spectroscopy simulation were using TD-DFT method at the same calculation level. These calculations were performed with the Gaussian 09 program package.[4]

2. Synthetic Procedures of 2 and 3

Synthesis of 2.

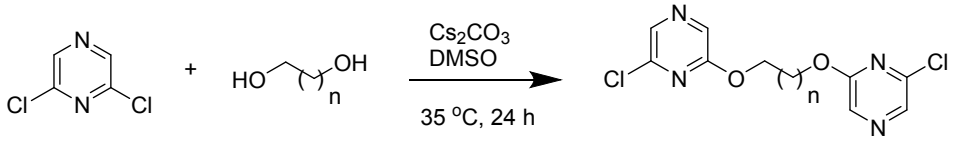

2a, n = 3;
2b, n = 5;
2c, n = 7;
2d, n = 9.

2a: A mixture of 2,6-dichloropyrazine (1.04 g, 7.00 mmol), Cs_2CO_3(2.28 g, 7.00 mmol) and 1,4-butanediol (0.18 ml, 2 mmol) in DMSO (100 mL) was stirred at 35 ºC for 24 h, poured into an aqueous HCl solution (1.0 M, 100 mL) and extracted with ethyl acetate (3 × 50 mL). The organic phases were combined, washed with brine, and concentrated under reduced pressure. The resulting residue was subjected to silica gel column chromatography (EtOAc/petroleum ether = 1:100) to afford 2a as a white solid (yield 60%). ^{1}H NMR (400 MHz, $CDCl_3$) δ 8.13 (s, 2H), 8.11 (s, 2H), 4.40 (t, J = 5.2 Hz, 4H), 2.01-1.93 (4H); ^{13}C NMR (100 MHz, $CDCl_3$) δ 159.3, 145.4, 135.2, 133.1, 66.7, 25.3. HRMS *m/z* $[M + H]^+$ calcd for $C_{12}H_{13}Cl_2N_4O_2$ 315.0410, found 315.0405.

2b: A white solid (yield 59%). ^{1}H NMR (400 MHz, $CDCl_3$) δ 8.12 (s, 2H), 8.10 (s, 2H), 4.33 (t, J = 6.6 Hz, 4H), 1.85-1.78 (m, 4H), 1.55-1.49 (4H); ^{13}C NMR (100 MHz,

$CDCl_3$,) δ 157.9, 143.9, 133.4, 131.6, 65.6, 27.0, 24.1. HRMS *m/z* $[M + H]^+$ calcd for $C_{14}H_{17}Cl_2N_4O_2$ 343.0723, found 343.0719.

2c: A white solid (yield: 70%). ^1H NMR (400 MHz, $CDCl_3$) δ 8.11 (s, 2H), 8.10 (s, 2H), 4.31 (t, *J* = 6.6 Hz, 4H), 1.82-1.75 (4H), 1.49-1.36 (8H); ^{13}C NMR (100MHz, $CDCl_3$) δ 159.5 145.4, 134.9, 133.2, 67.3, 29.2, 28.6, 25.8. HRMS *m/z* $[M + H]^+$ calcd for $C_{16}H_{21}Cl_2N_4O_2$ 371.1036, found 371.1032.

2d: A white solid (yield 67%). ^1H NMR (400 MHz, $CDCl_3$) δ 8.11 (s, 2H), 8.10 (s, 2H), 4.31 (t, *J* = 6.7 Hz, 4H), 1.81-1.74 (4H), 1.45-1.32 (12H); ^{13}C NMR (100 MHz, $CDCl_3$) δ 159.5, 145.4, 134.9, 133.2, 67.4, 29.4, 29.3, 28.6, 25.9. HRMS *m/z* $[M + H]^+$ calcd for $C_{18}H_{25}Cl_2N_4O_2$ 399.1349, found 399.1343.

Synthesis of 3.

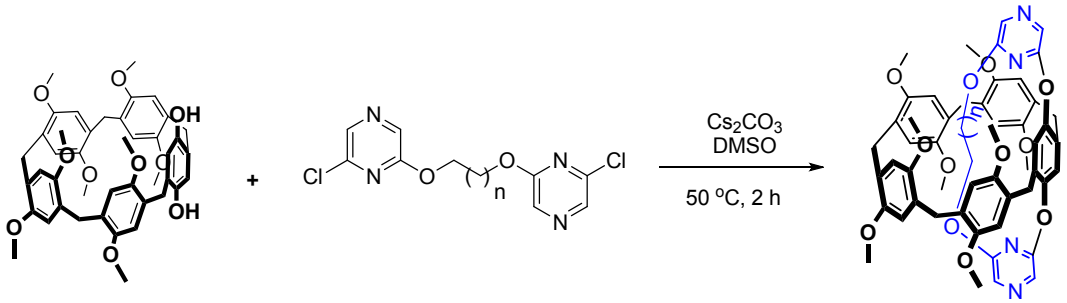

1

2a, n = 3
2b, n = 5
2c, n = 7
2d, n = 9

3a, n = 3
3b, n = 5
3c, n = 7
3d, n = 9

3a: A mixture of **1** (361.0 mg, 0.5 mmol), Cs_2CO_3(652.0 mg, 2.0 mmol) and **2a** (189 mg, 0.6 mmol) in DMSO (50 mL) was heated to 50 ºC under nitrogen for 2 h, poured into an aqueous HCl solution (1.0 M, 50 mL), and extracted with EtOAc (3 × 25 mL). The organic phases were combined, washed with brine, and concentrated under reduced pressure. The resulting residue was subjected to silica gel column chromatography (EtOAc/petroleum ether = 1:5) to afford **3a** as a white solid (yield 34%). ^1H NMR (600 MHz, $CDCl_3$) δ 8.12 (s, 2H), 7.69 (s, 2H), 7.26 (s, 2H), 7.05 (s, 2H), 6.81 (s, 2H), 6.73 (s, 2H), 5.76 (s, 2H), 3.90-3.83 (16H), 3.74-3.68 (6H), 3.39 (s, 6H), 3.08 (s, 6H), 2.48-2.44 (2H), 2.02-1.95 (2H), -1.22 (m, 2H), -1.80 (m, 2H); ^{13}C NMR (150 MHz, $CDCl_3$) δ 159.2, 158.3, 150.9, 150.4, 150.0, 149.9, 147.0, 132.1, 129.2, 128.4, 128.4, 126.2, 125.9, 125.8, 122.9, 113.8, 113.5, 113.1, 113.0, 67.6, 55.4, 55.0, 54.9, 54.4, 30.0, 29.5, 28.2, 19.9. HRMS *m/z* $[M + H]^+$ calcd for $C_{55}H_{57}N_4O_{12}$ 965.3967, found 965.3963.

3b: A white solid (yield 38%). ^{1}H NMR (600 MHz, $CDCl_3$) δ 8.10 (s, 2H), 7.86 (s, 2H), 7.11 (s, 2H), 6.95 (s, 2H), 6.87 (s, 2H), 6.77 (s, 2H), 6.15 (s, 2H), 3.87-3.77 (18H), 3.74-3.70 (4H), 3.55 (s, 6H), 3.37-3.31(2H), 3.26-3.20 (2H), 3.04 (s, 6H), 0.03 (m, 2H), -0.15 (m, 2H), -2.12 (m, 2H), -2.24 (m, 2H); ^{13}C NMR (150 MHz, $CDCl_3$) δ 158.5, 157.7, 150.6, 150.5, 150.3, 150.1, 146.9, 132.1, 128.3, 128.0, 127.9, 127.2, 124.3, 123.7, 114.2, 113.5, 113.3, 112.4, 67.7, 55.5, 55.3, 55.2, 53.9, 29.3, 29.2, 29.0, 27.1, 21.6. HRMS *m/z* $[M + H]^+$ calcd for $C_{57}H_{61}N_4O_{12}$, 993.4280, found 993.4278.

3c: A white solid (yield 41%). ^{1}H NMR (600 MHz, $CDCl_3$) δ 8.07 (s, 2H), 7.87 (s, 2H), 7.03 (s, 2H), 6.95 (s, 2H), 6.90 (s, 2H), 6.74 (s, 2H), 6.32 (s, 2H), 3.83-3.78 (16H), 3.75-3.69 (6H), 3.63-3.58 (2H), 3.48 (s, 6H), 3.41 (s, 6H), 3.32-3.27 (m, 2H), 0.25-0.12 (m, 6H), -0.42 (m, 2H), -0.59 (m, 4H); ^{13}C NMR (150 MHz, $CDCl_3$) δ 159.4, 157.5, 150.5, 150.3, 150.3, 150.1, 148.3, 130.5, 128.8, 128.2, 128.1, 127.7, 126.3, 125.4, 120.7, 113.7, 113.6, 113.2, 113.1, 65.9, 55.4, 55.1, 55.0, 55.0, 29.5, 29.3, 28.7, 28.6, 27.9, 23.8. HRMS *m/z* $[M + H]^+$ calcd for $C_{59}H_{65}N_4O_{12}$ 1021.4593, found 1021.4594.

3d: A white solid (yield 32%). ^{1}H NMR (600 MHz, $CDCl_3$) δ 7.86 (s, 2H), 7.83 (s, 2H), 7.19 (s, 2H), 6.95 (s, 2H), 6.90 (s, 2H), 6.80 (s, 2H), 6.26 (s, 2H), 3.87 – 3.74 (20H), 3.67-3.62 (2H), 3.62-3.58 (2H), 3.53 (s, 6H), 3.51 (s, 6H), 3.33-3.26 (2H), 0.91-0.83 (2H), 0.71-0.62 (2H), 0.50-0.40 (2H), 0.33-0.16 (6H), (-0.30)-(-0.54) (4H); ^{13}C NMR (150 MHz, $CDCl_3$) δ 159.1, 158.9, 150.4, 150.3, 150.1, 150.1, 148.2, 132.4, 129.0, 128.3, 128.0, 127.4, 125.8, 124.2, 123.0, 113.8, 113.2, 113.1, 112.9, 66.4, 55.2, 55.2, 55.0, 54.7, 30.6, 29.8, 29.7, 28.8, 28.7, 25.8, 23.4. HRMS *m/z* $[M + H]^+$ calcd for $C_{61}H_{69}N_4O_{12}$ 1049.4907, found 1049.4906.

3. Crystallographic Data of 3

3a: $C_{55}H_{56}N_4O_{12}$, M_r = 965.04, T =296(2) K, Monoclinic, space group $P2(1)/c$, a = 21.1000(11), b =23.1109(12), c = 23.2010(12) Å, $\alpha = \gamma = 90°$, β= 112.784(2)°, V =10430.9(9) Å^3, Z = 8, ρcalcd. = 1.229 g/cm^3, crystal size = 0.48×0.42×0.18 mm, μ = 0.087 mm^{-1}, reflections collected 121362, unique reflections 18375, data/restraints/parameters 18375/1/1279, GOF on F^2 1.069, R_{int} for independent data 0.0558, final R_1 = 0.0532, wR_2 = 0.1427, R indices (all data): R_1 = 0.0962, wR_2 = 0.1586, largest diff. peak and hole: 0.277 and -0.175 e/Å^3.

3b: $C_{57}H_{60}N_4O_{12}$, M_r = 993.09, T =296(2) K, triclinic, space group P-1, a = 12.3460(5), b =19.5371(7), c = 22.8661(9) Å, α = 106.5610(10)°, β= 102.4580(10)°, γ =

97.1470(10)°, V =5059.3(3) Å^3, Z = 4, ρcalcd. = 1.304 g/cm^3, crystal size = 0.41×0.40×0.19 mm, μ = 0.092 mm^{-1}, reflections collected 59757, unique reflections 17744, data/restraints/parameters 17744/8/1315, GOF on F^2 1.029, R_{int} for independent data 0.0452, final R_1 = 0.0580, wR_2 = 0.1453, R indices (all data): R_1 = 0.1031, wR_2 = 0.1776, largest diff. peak and hole: 0.764 and -0.470 e/Å^3.

G ⊂ 3b: $C_{63}H_{68}N_6O_{12}$, M_r = 1101.23, T =293(2) K, Orthorhombic, space group *Pbca*, a = 20.9082(3), b =23.7424(4), c = 23.9838(4) Å, $\alpha = \beta = \gamma = 90°$, V =11905.8(3) Å^3, Z = 8, ρcalcd. = 1.229 g/cm^3, crystal size = 0.48×0.42×0.36 mm, μ = 0.698 mm^{-1}, reflections collected 75376, unique reflections 11202, data/restraints/parameters 11202/1410/731, GOF on F^2 1.436, R_{int} for independent data 0.0442, final R_1 = 0.1012, wR_2 = 0.3309, R indices (all data): R_1 = 0.1236, wR_2 = 0.3593, largest diff. peak and hole: 1.135 and -0.925 e/Å^3.

3c: $C_{59}H_{64}N_4O_{12}$, M_r = 1021.14, T =293(2) K, monoclinic, space group *P* 1 21/c 1, a = 11.54060(10), b =19.4516(2), c = 23.9649(2) Å, $\alpha = \gamma = 90°$, β= 101.4550(10)°, V =5272.56(9) Å^3, Z = 4, ρcalcd. = 1.286 g/cm^3, crystal size = 0.48×0.41×0.32 mm, μ = 0.735 mm^{-1}, reflections collected 143580, unique reflections 10739, data/restraints/parameters 10739/0/685, GOF on F^2 1.042, R_{int} for independent data 0.0591, final R_1 = 0.0436, wR_2 = 0.1176, R indices (all data): R_1 = 0.0522, wR_2 = 0.1226, largest diff. peak and hole: 0.220 and -0.174 e/Å^3.

DCM ⊂ 3c: $C_{61}H_{68}Cl_4N_4O_{12}$, M_r = 1190.99, T =296(2) K, triclinic, space group *P*-1, a = 11.0365(7), b =16.7007(10), c = 17.2058(10) Å, α = 93.872(2)°, β= 92.106(2)°, γ = 108.051(2)°, V =3002.8(3)Å^3, Z = 2, ρcalcd. = 1.317 g/cm^3, crystal size = 0.36×0.32×0.28 mm, μ = 0.261 mm^{-1}, reflections collected 35309, unique reflections 10513, data/restraints/parameters 10513/0/730, GOF on F^2 1.018, R_{int} for independent data 0.0403, final R_1 = 0.0896, wR_2 = 0.2567, R indices (all data): R_1 = 0.1276, wR_2 = 0.2999, largest diff. peak and hole: 0.767 and -0.885 e/Å^3.

3d: $C_{61}H_{68}N_4O_{12}$, M_r = 1049.19, T =296(2) K, monoclinic, space group *P*2(1)/n, a = 11.9894(6), b =21.2887(10), c = 21.7173(11) Å, $\alpha = \gamma = 90°$, β= 93.300(2)°, V =5533.9(5) Å^3, Z = 4, ρcalcd. = 1.259 g/cm^3, crystal size = 0.46×0.38×0.26 mm, μ = 0.088 mm^{-1}, reflections collected 64552, unique reflections 9755, data/restraints/parameters 9755/0/694, GOF on F^2 0.995, R_{int} for independent data 0.1194, final R_1 = 0.0521, wR_2 = 0.1071, R indices (all data): R_1 = 0.1511, wR_2 = 0.1492, largest diff. peak and hole: 0.149 and -0.203 e/Å^3.

4. ^{1}H NMR and ^{13}C NMR of 2

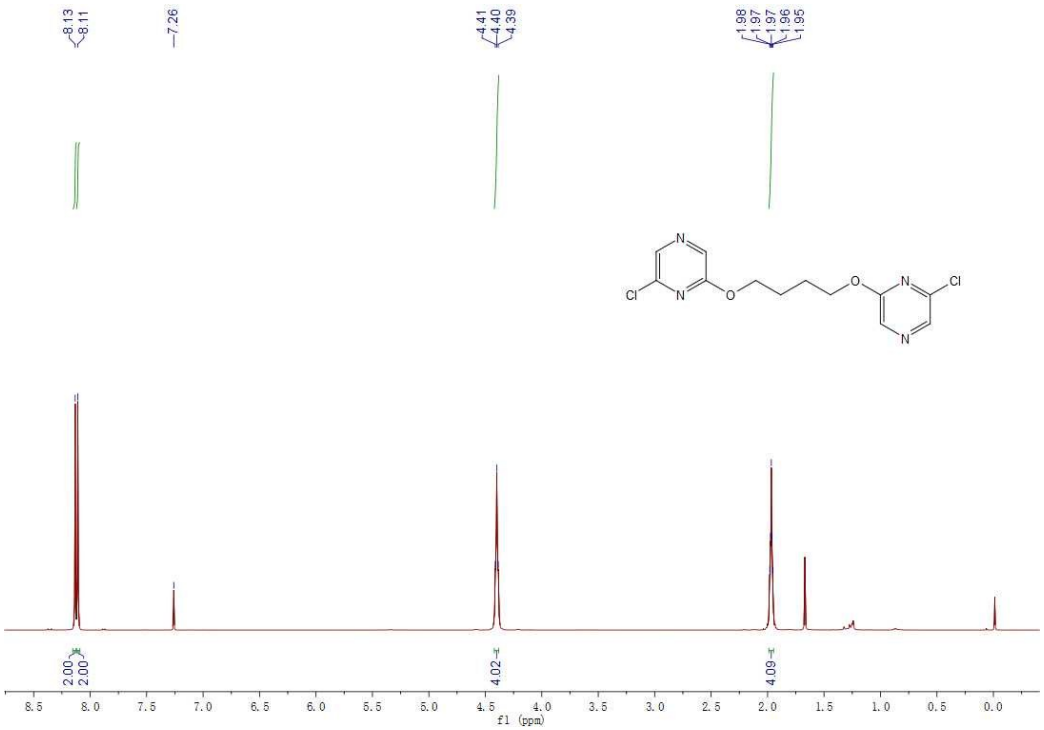

Fig. S1 ^{1}H NMR spectrum (400 MHz, $CDCl_3$) of compound **2a**.

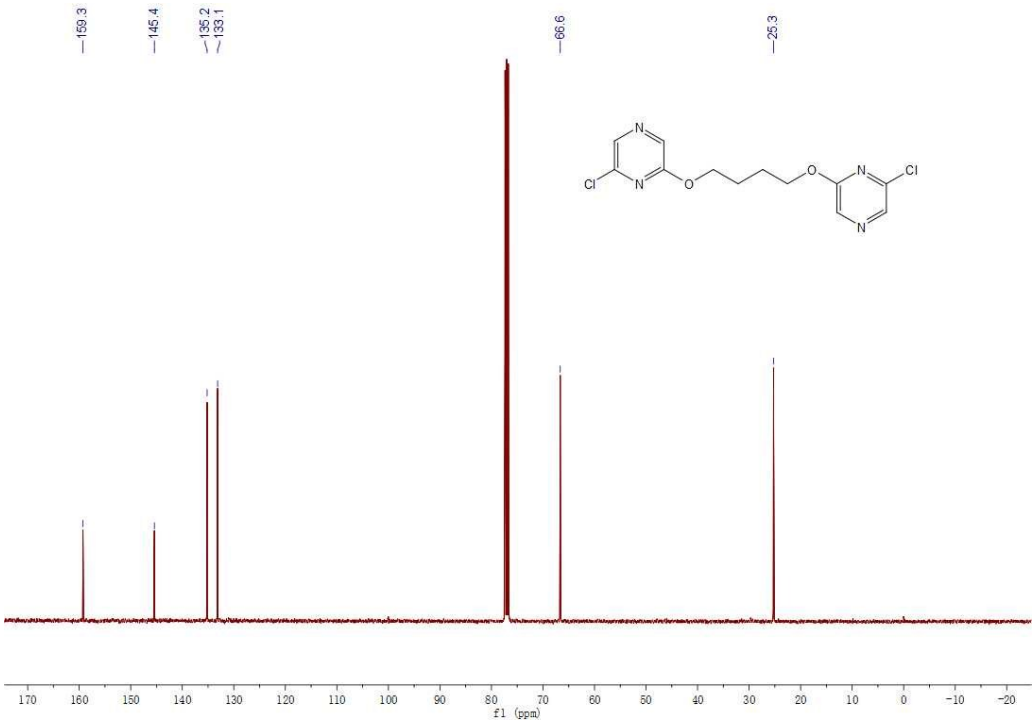

Fig. S2 ^{13}C NMR spectrum (100 MHz, $CDCl_3$) of compound **2a**.

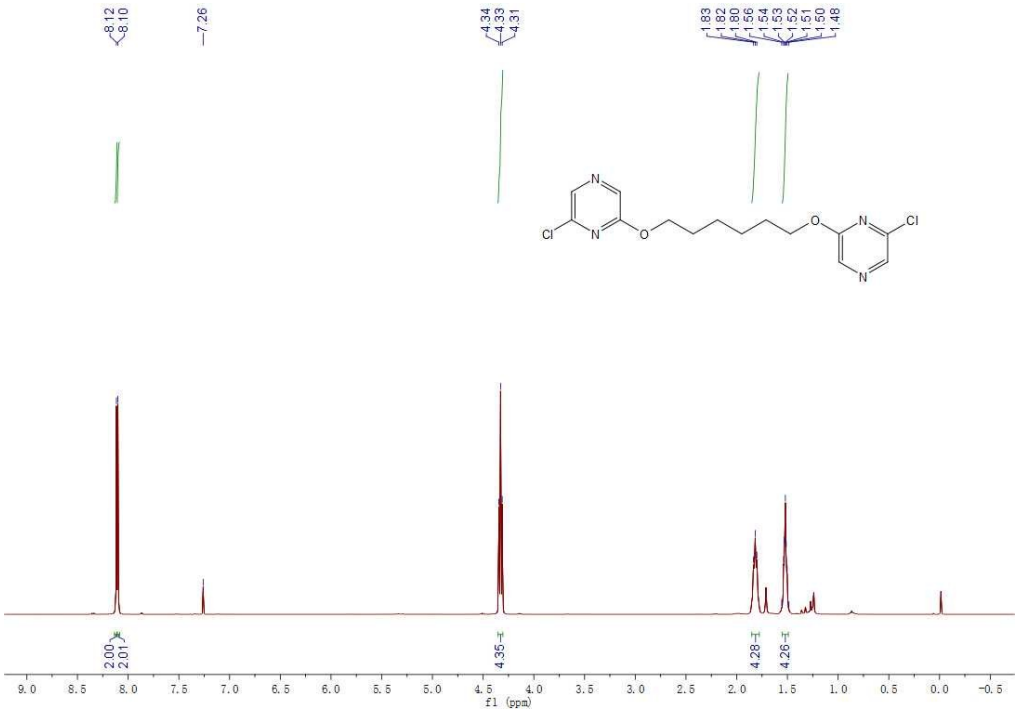

Fig. S3 ^{1}H NMR spectrum (400 MHz, $CDCl_3$) of compound **2b**.

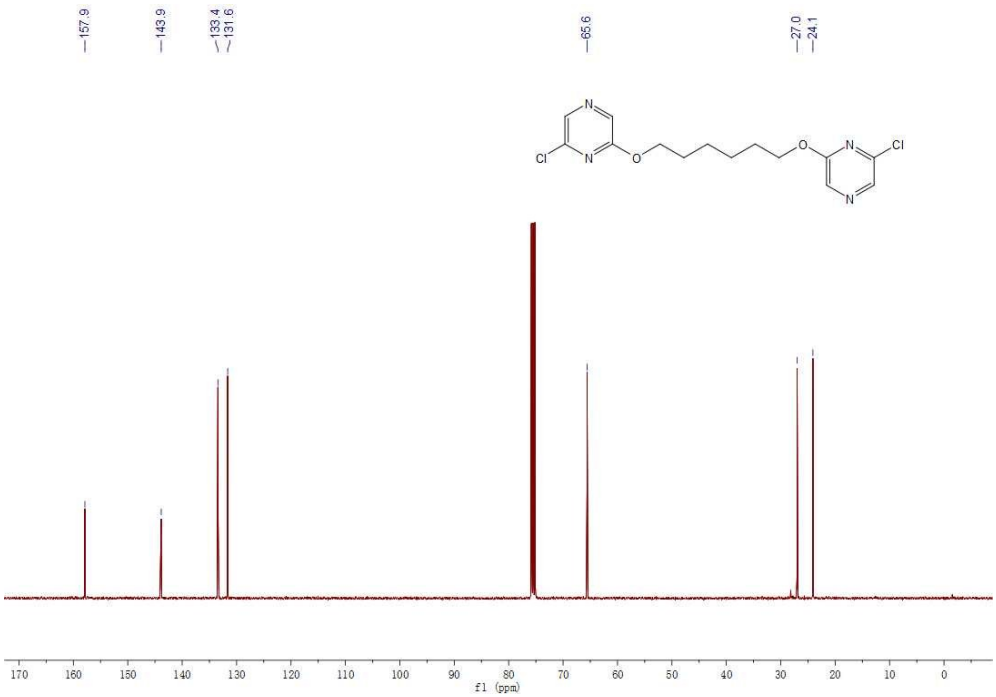

Fig. S4 ^{13}C NMR spectrum (100 MHz, $CDCl_3$) of compound **2b**.

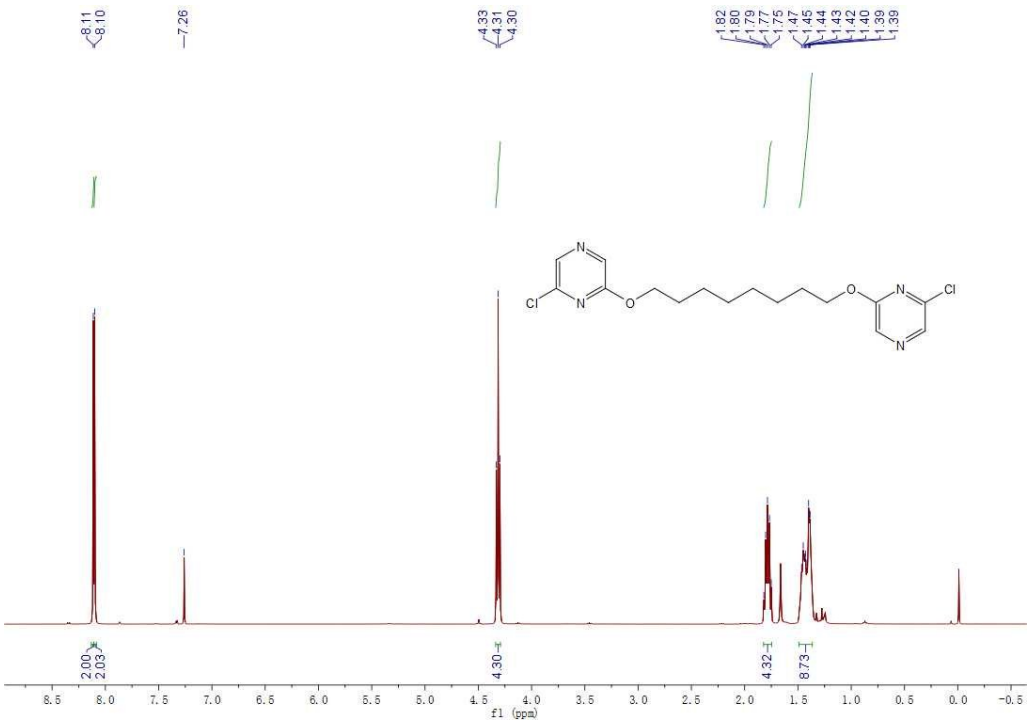

Fig. S5 ^{1}H NMR spectrum (400 MHz, $CDCl_3$) of compound **2c**.

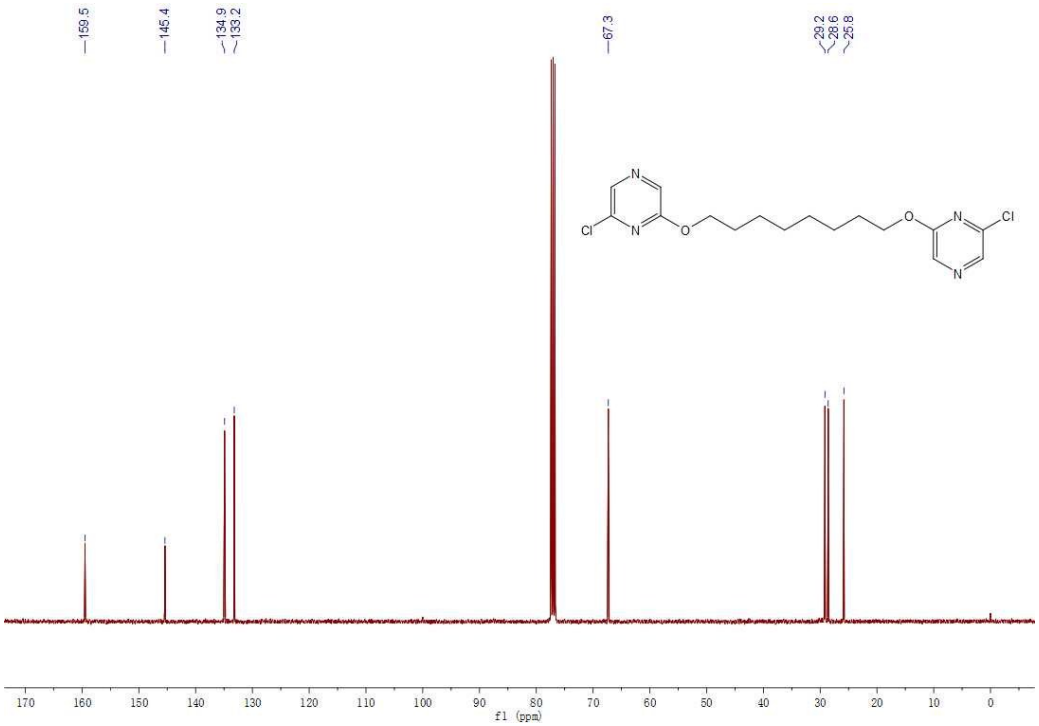

Fig. S6 ^{13}C NMR spectrum (100 MHz, $CDCl_3$) of compound **2c**.

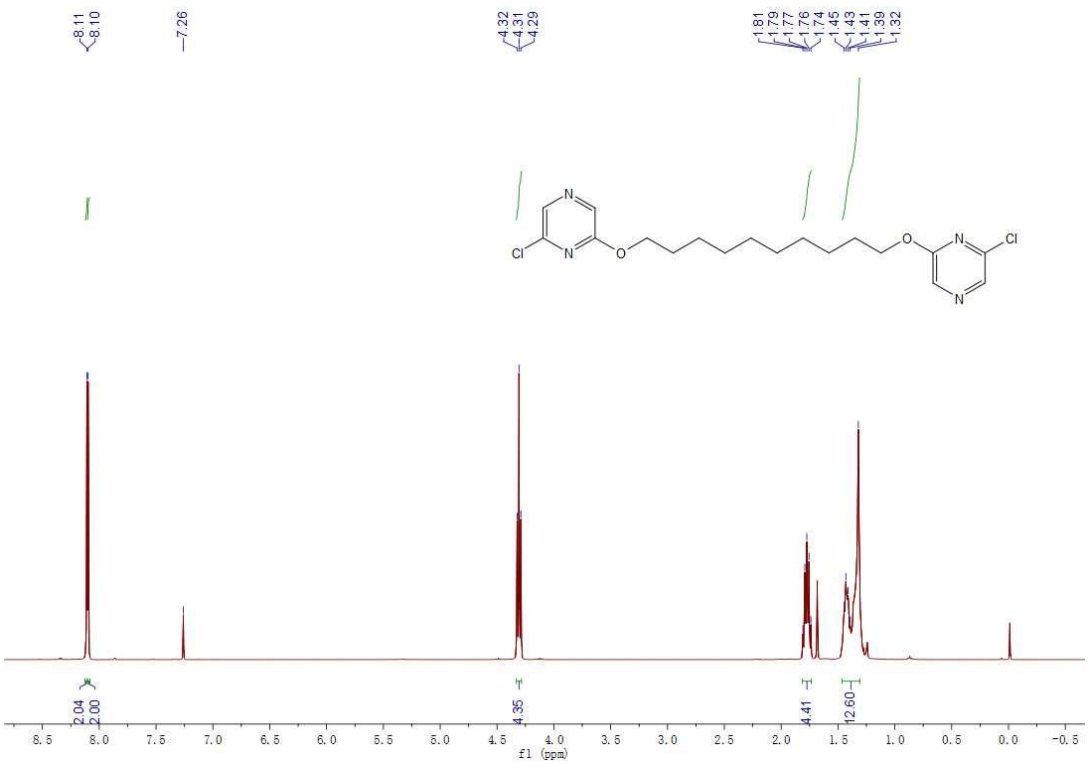

Fig. S7 ^{1}H NMR spectrum (400 MHz, $CDCl_3$) of compound **2d**.

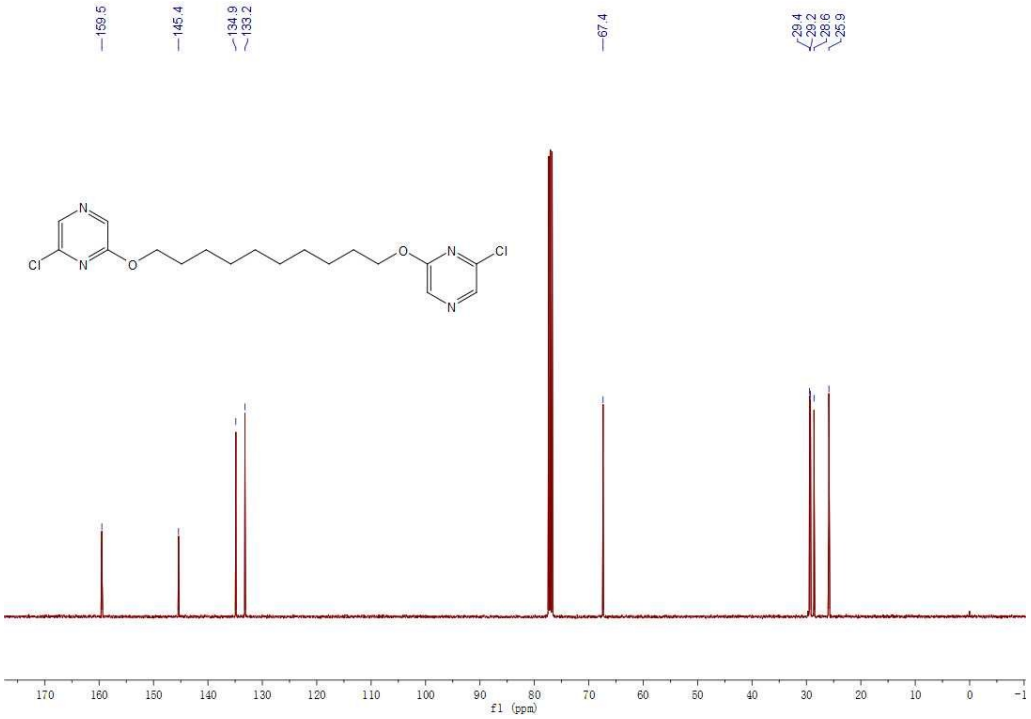

Fig. S8 ^{13}C NMR spectrum (100 MHz, $CDCl_3$) of compound **2d**.

5. ^{1}H NMR, ^{13}C NMR, 2D NOESY spectra and HRMS of 3

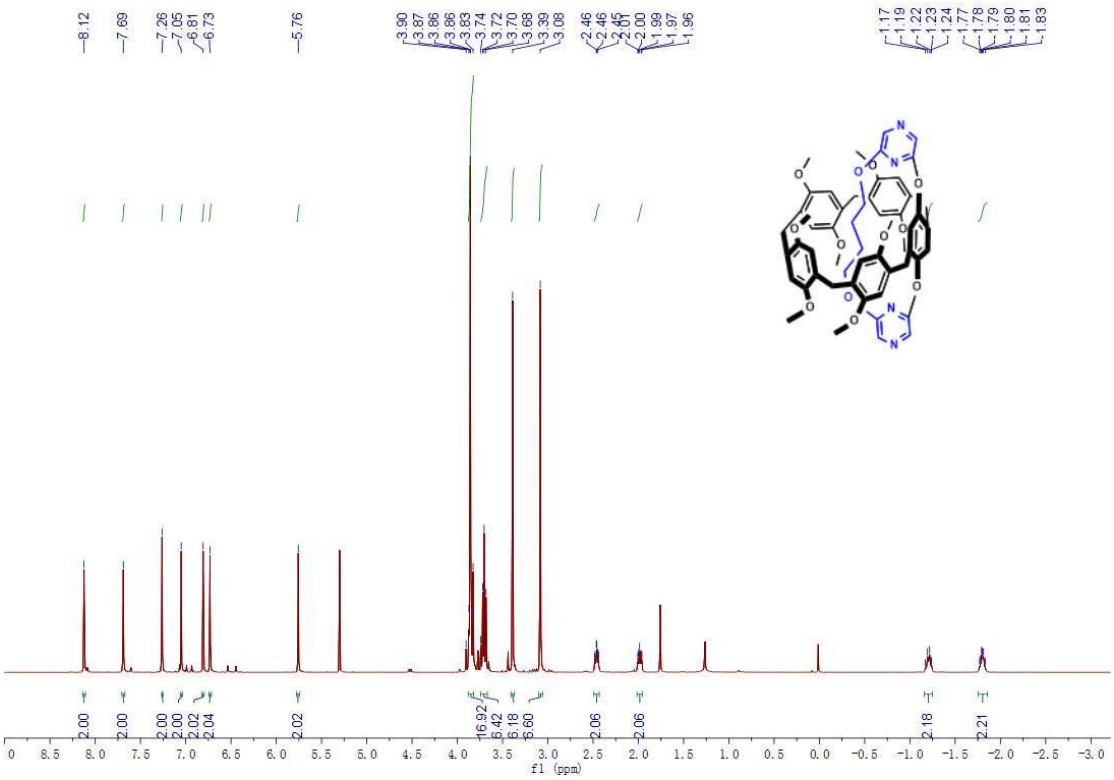

Fig. S9 ^{1}H NMR spectrum (600 MHz, $CDCl_3$) of compound **3a**.

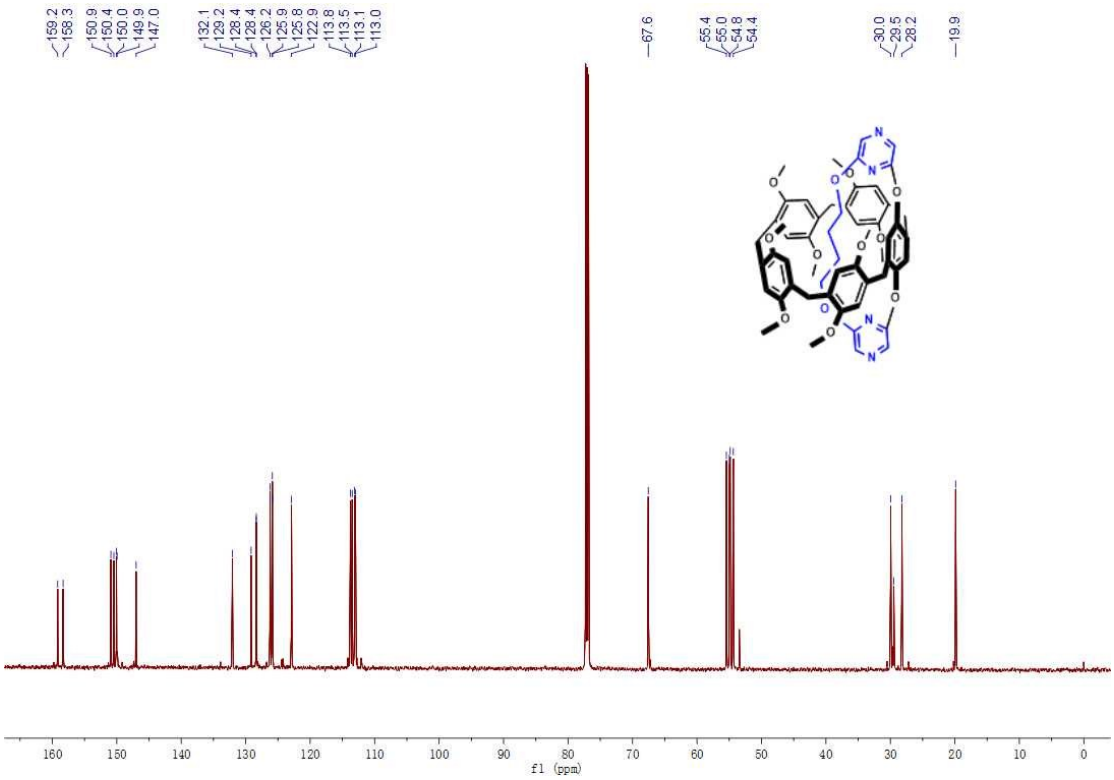

Fig. S10 ^{13}C NMR spectrum (150 MHz, $CDCl_3$) of compound **3a**.

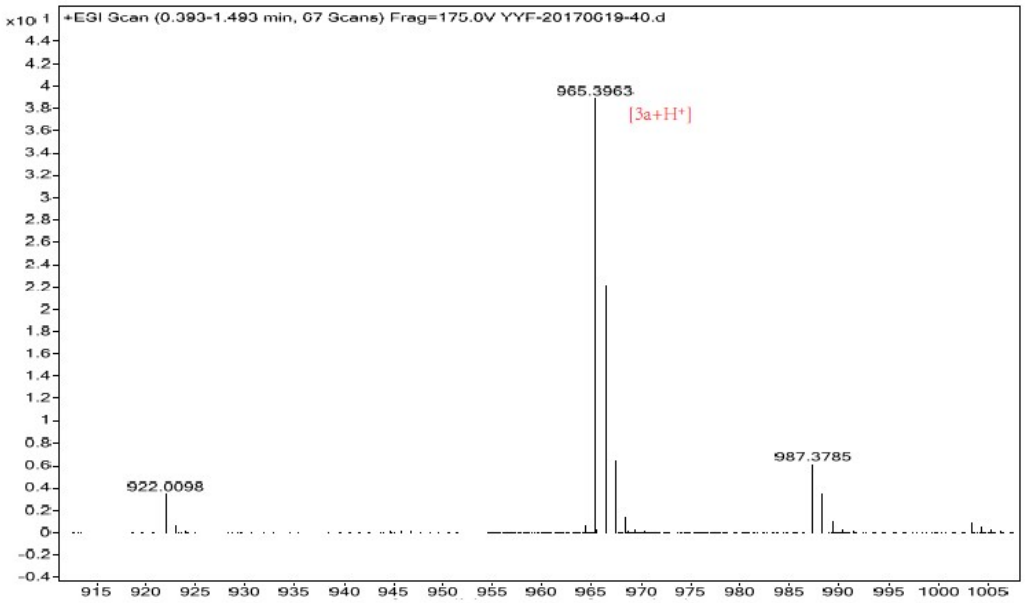

Fig. S11 ESI HRMS spectrum of compound **3a**.

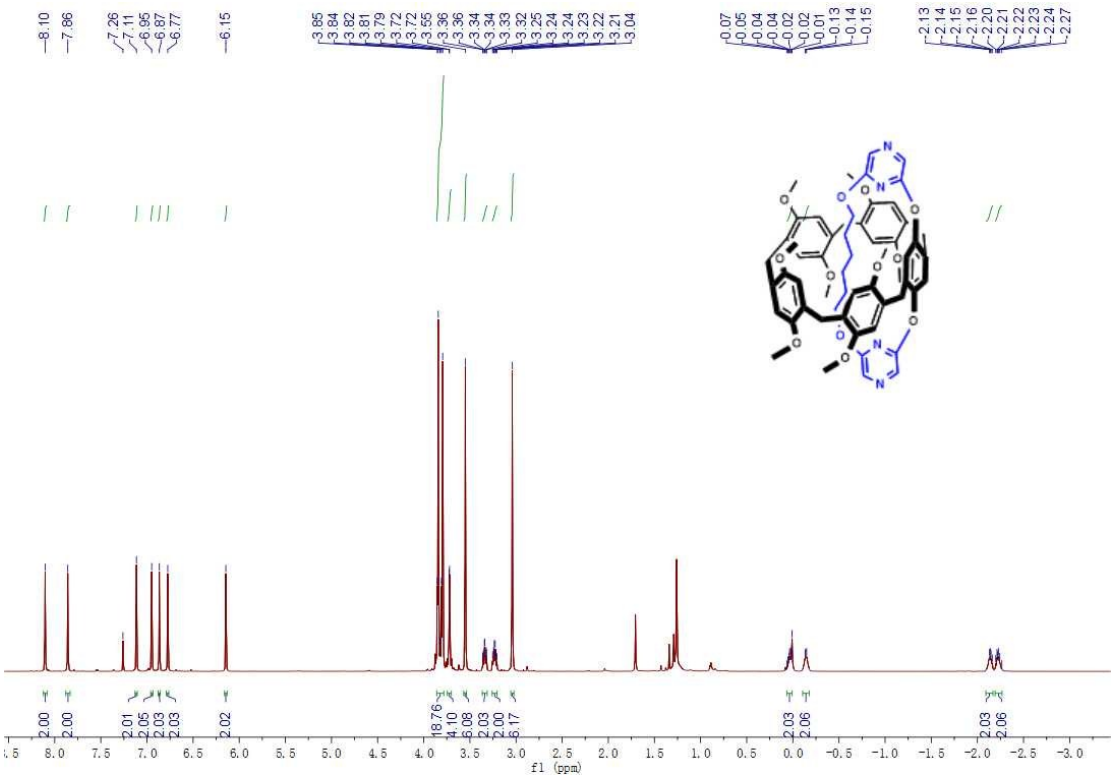

Fig. S12 ^{1}H NMR spectrum (600 MHz, $CDCl_3$) of compound **3b**.

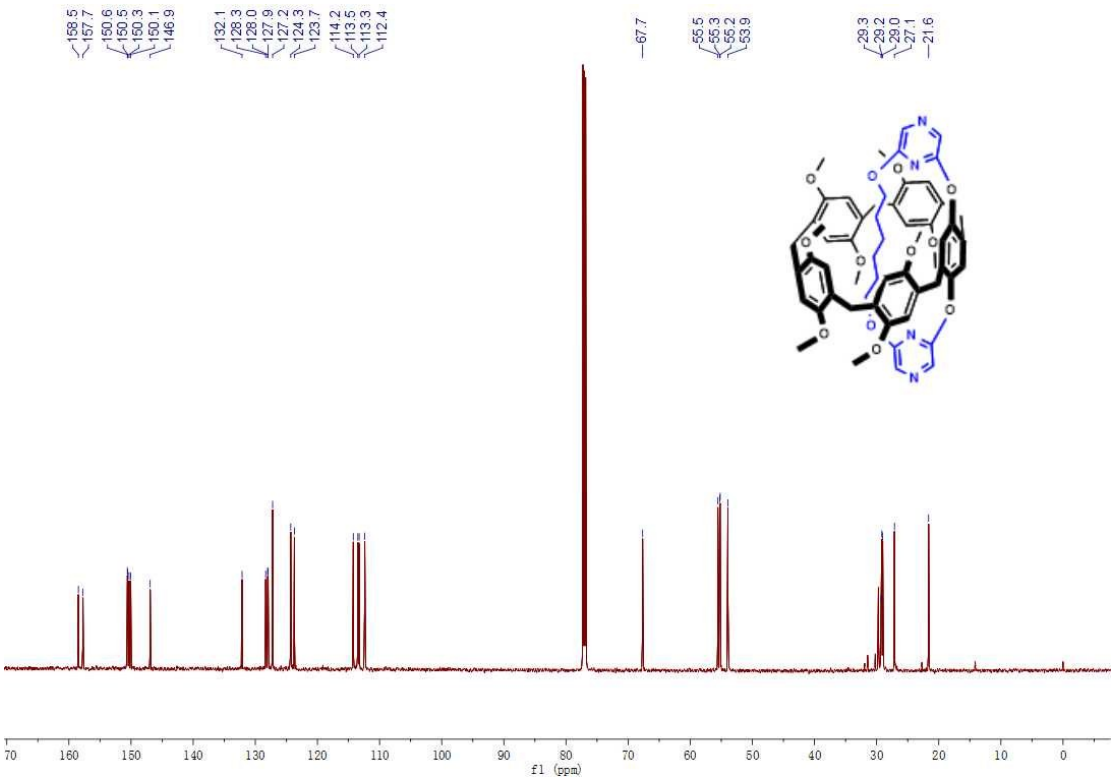

Fig. S13 ^{13}C NMR spectrum (150 MHz, $CDCl_3$) of compound **3b**.

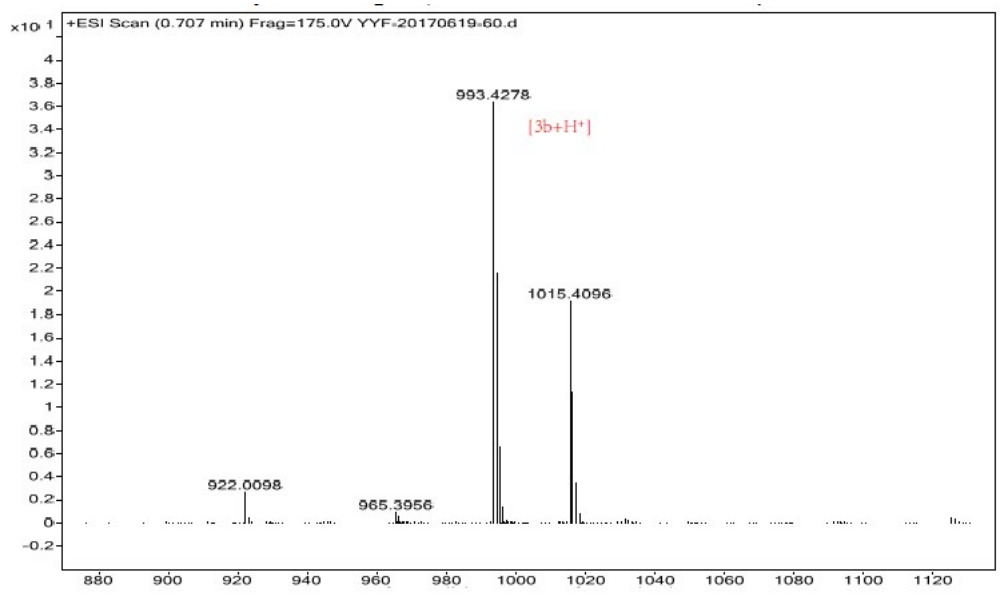

Fig. S14 ESI HRMS spectrum of compound **3b**.

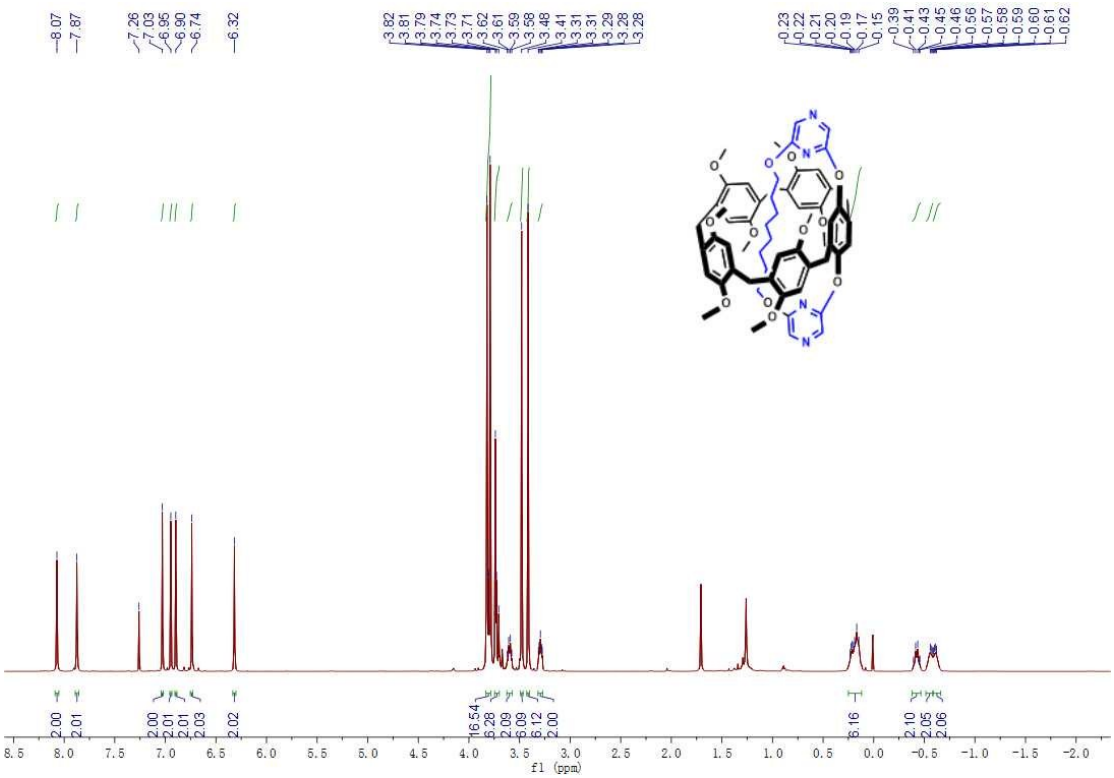

Fig. S15 ^{1}H NMR spectrum (600 MHz, $CDCl_3$) of compound **3c**.

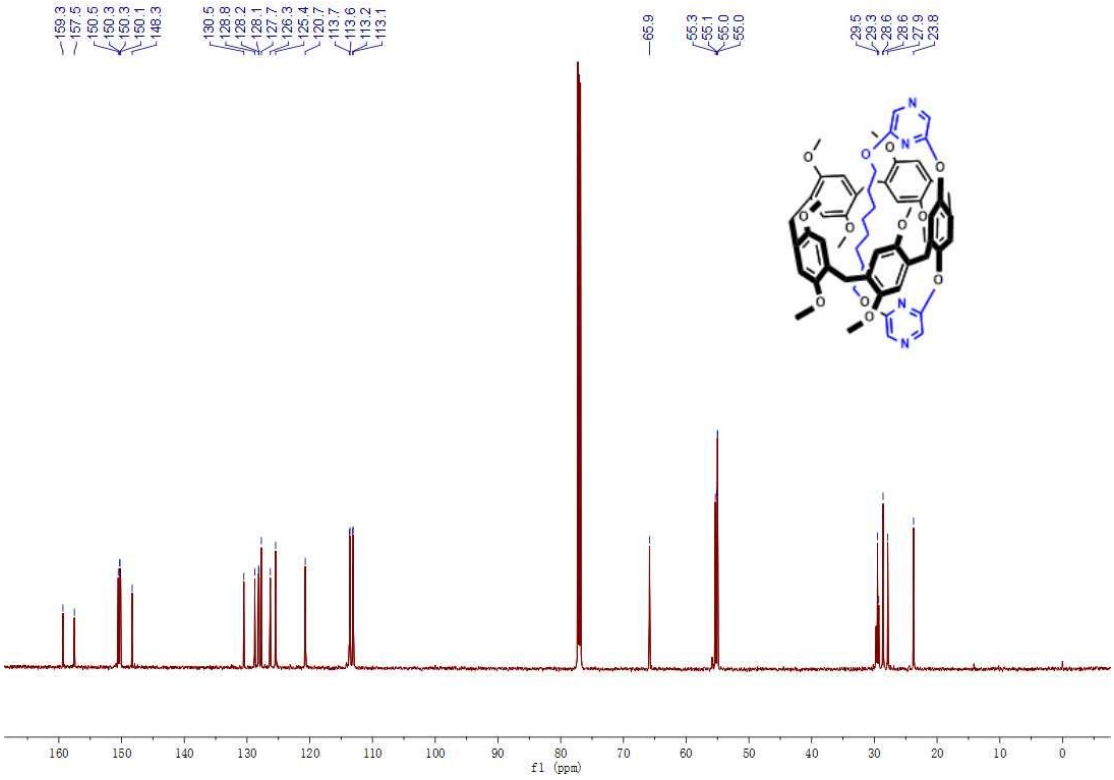

Fig. S16 ^{13}C NMR spectrum (150 MHz, $CDCl_3$) of compound **3c**.

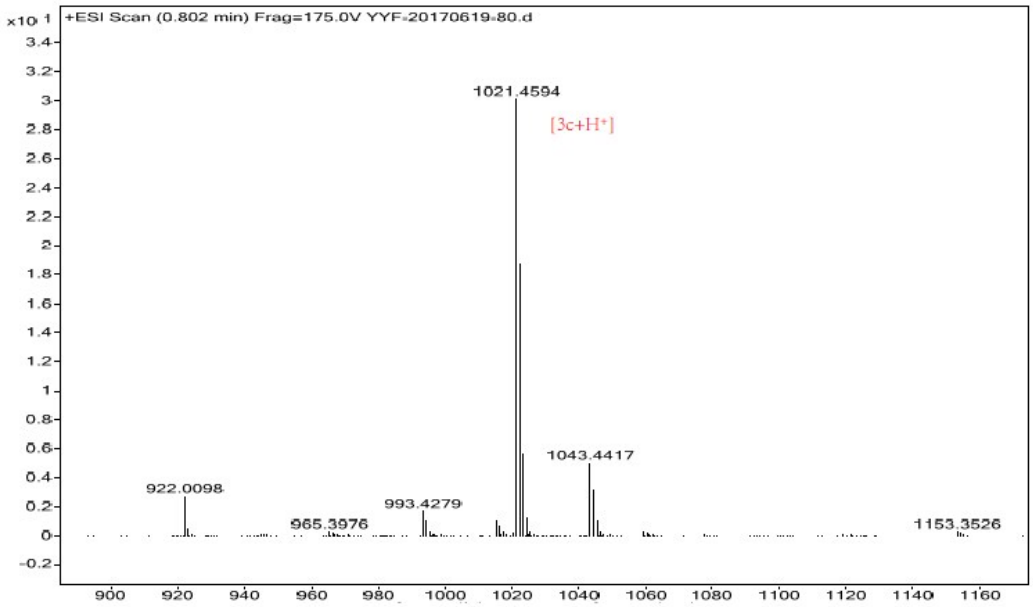

Fig. S17 ESI HRMS spectrum of compound **3c**.

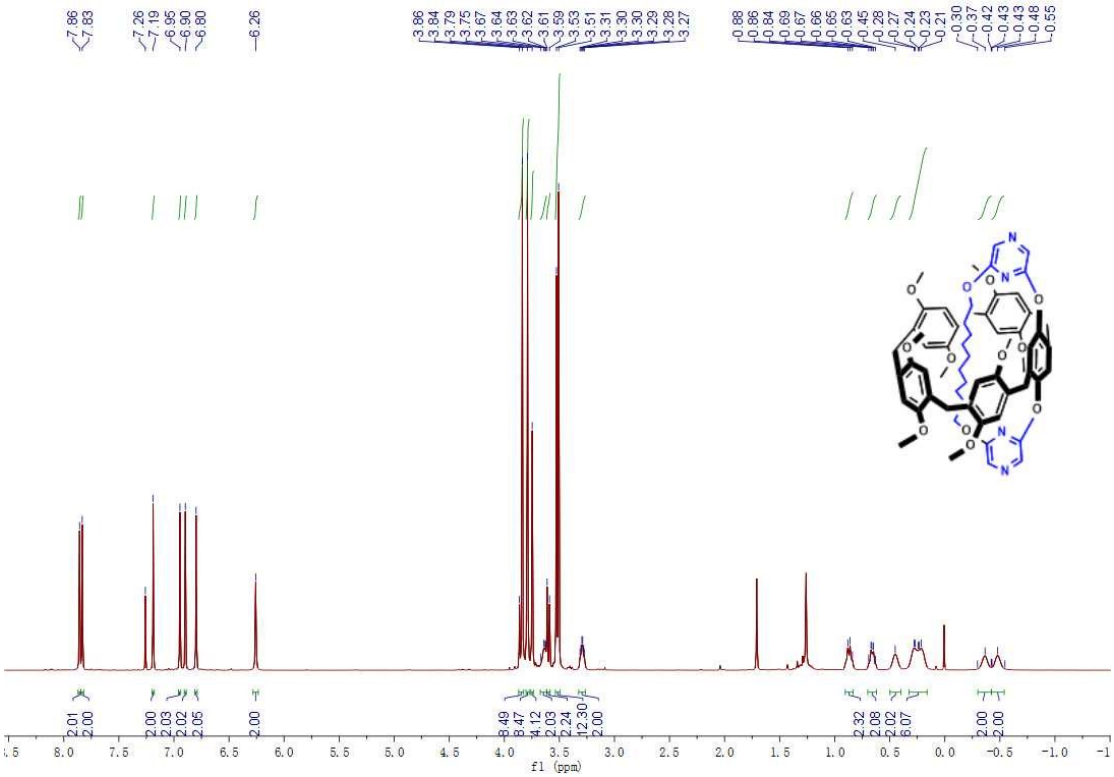

Fig. S18 ^{1}H NMR spectrum (600 MHz, $CDCl_3$) of compound **3d**.

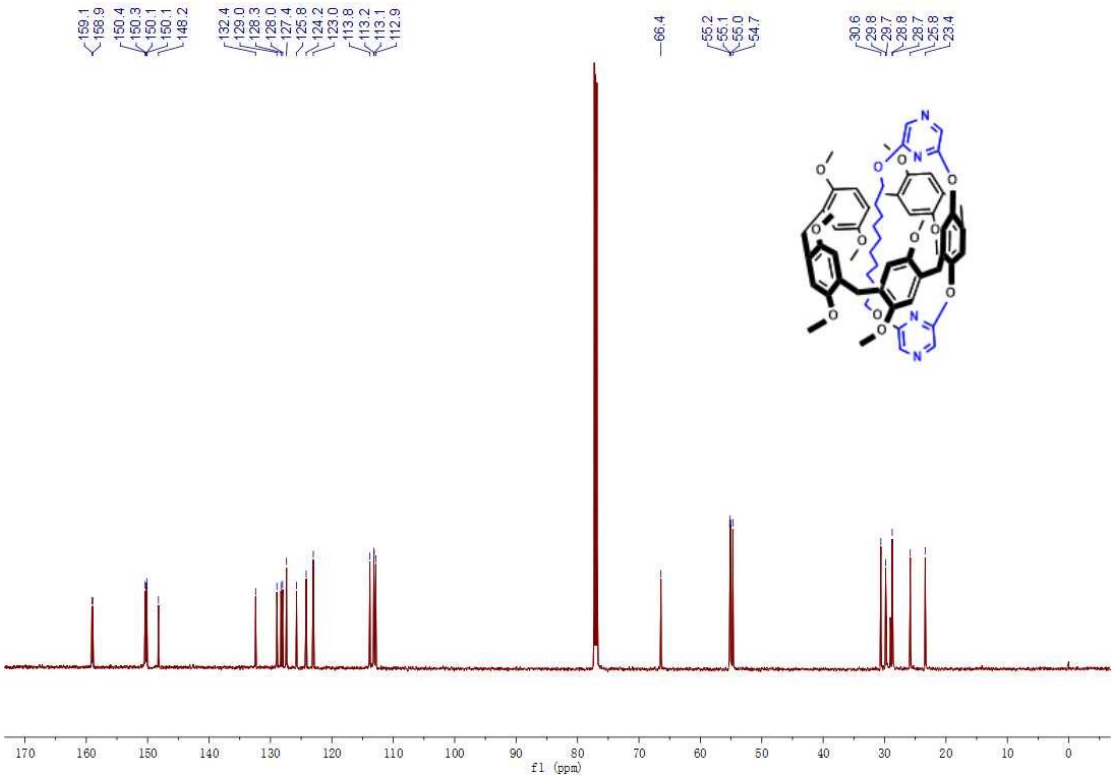

Fig. S19 ^{13}C NMR spectrum (150 MHz, $CDCl_3$) of compound **3d**.

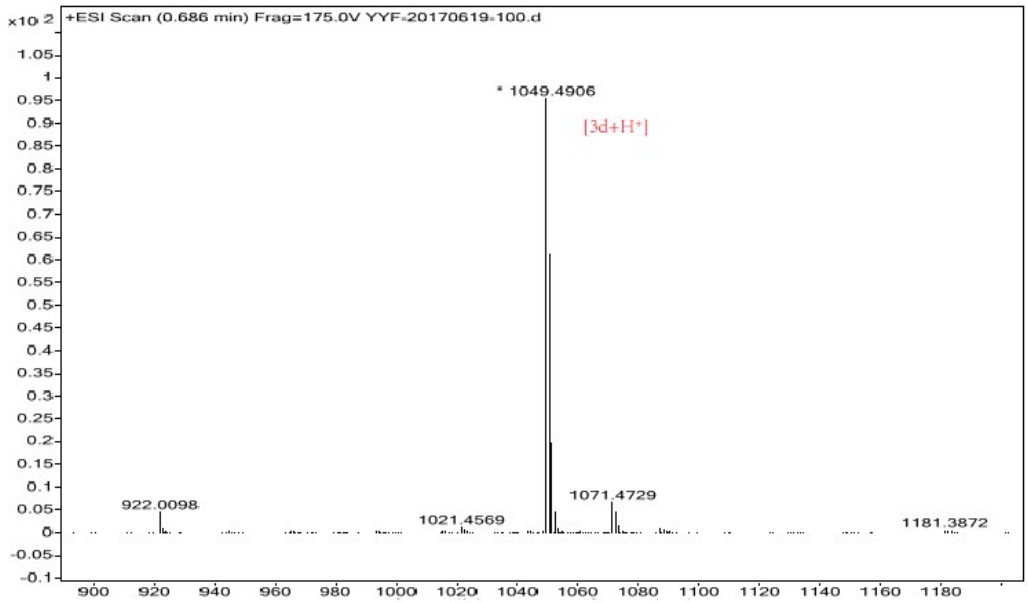

Fig. S20 HRMS spectrum of compound **3d**.

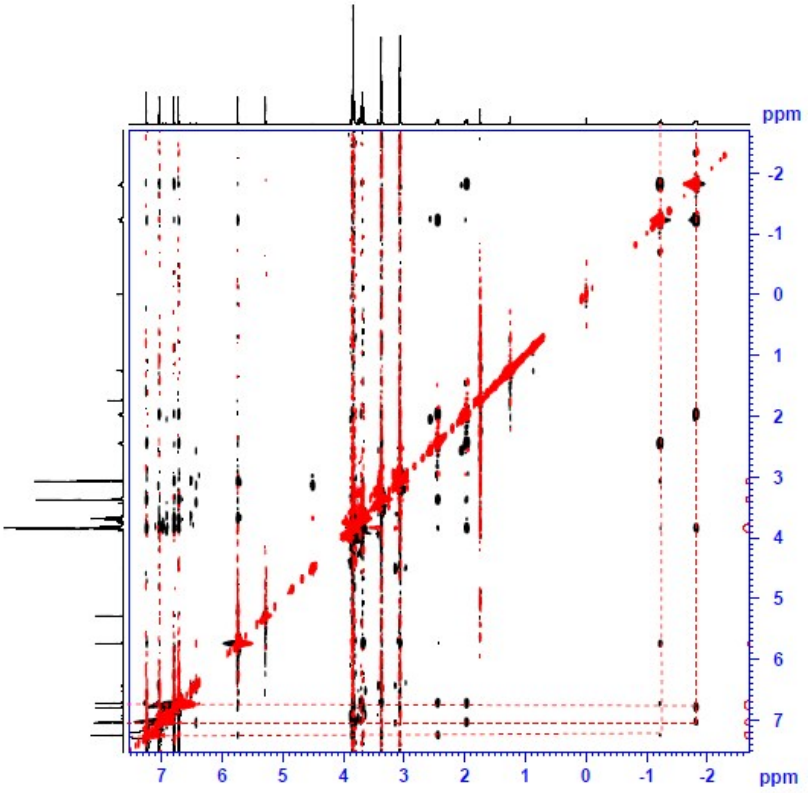

Fig. S21 2D NOESY spectrum of **3a** in $CDCl_3$ (600 MHz, 298 K).

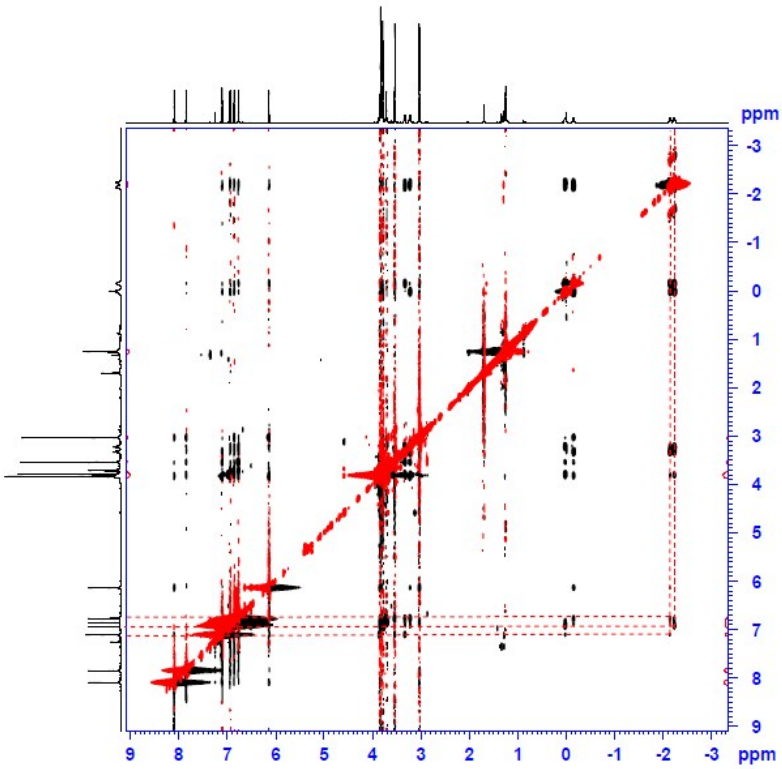

Fig. S22 2D NOESY spectrum of **3b** in $CDCl_3$ (600 MHz, 298 K).

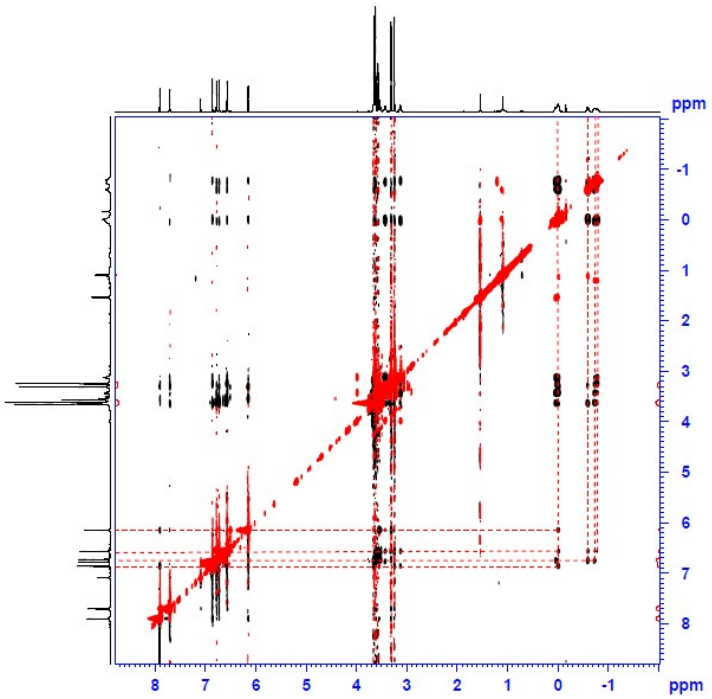

Fig. S23 2D NOESY spectrum of **3c** in $CDCl_3$ (600 MHz, 298 K).

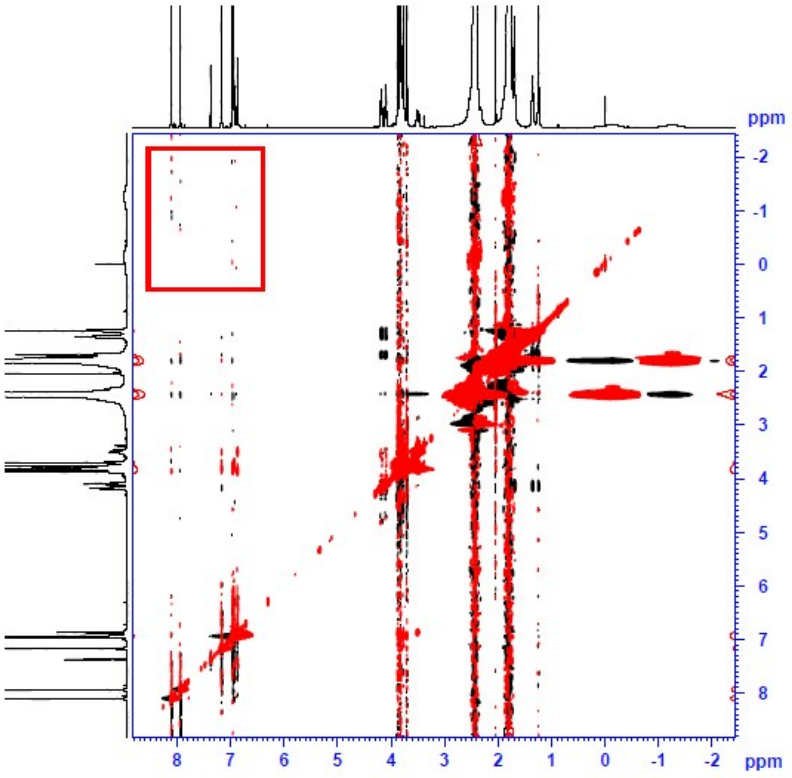

Fig. S24 2D NOESY spectrum of **3c** with access **G** in $CDCl_3$ (600 MHz, 298 K).

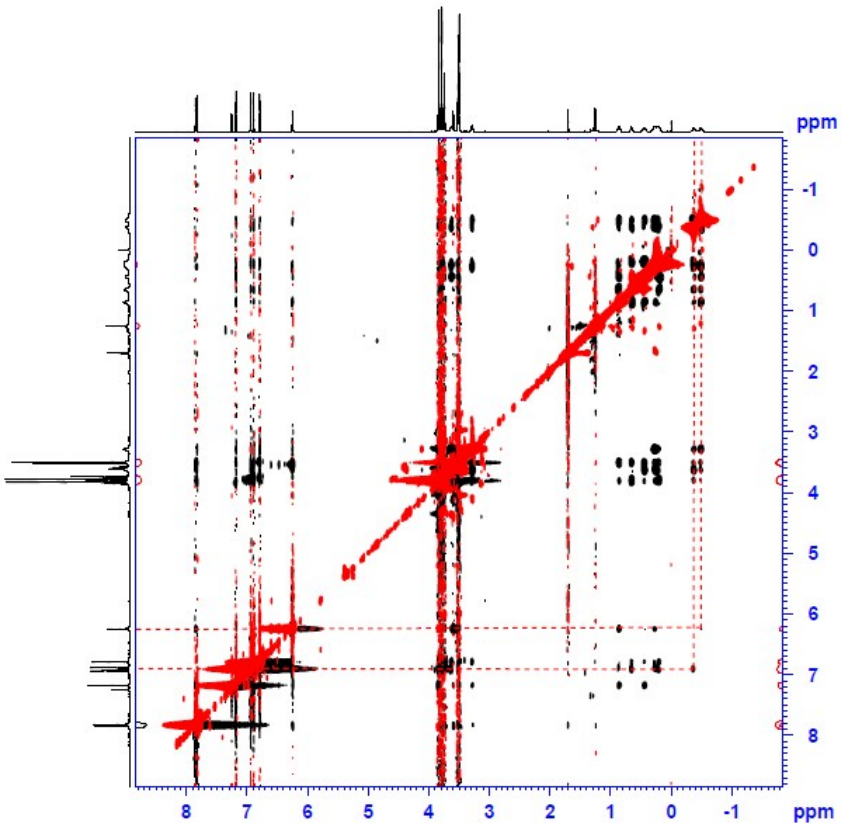

Fig. S25 2D NOESY spectrum of **3d** in $CDCl_3$ (600 MHz, 298 K).

6. ^{1}H NMR for 3 in $CDCl_3$, CD_2Cl_2 and $CDCl_3$-CD_2Cl_2 (1:1, v/v)

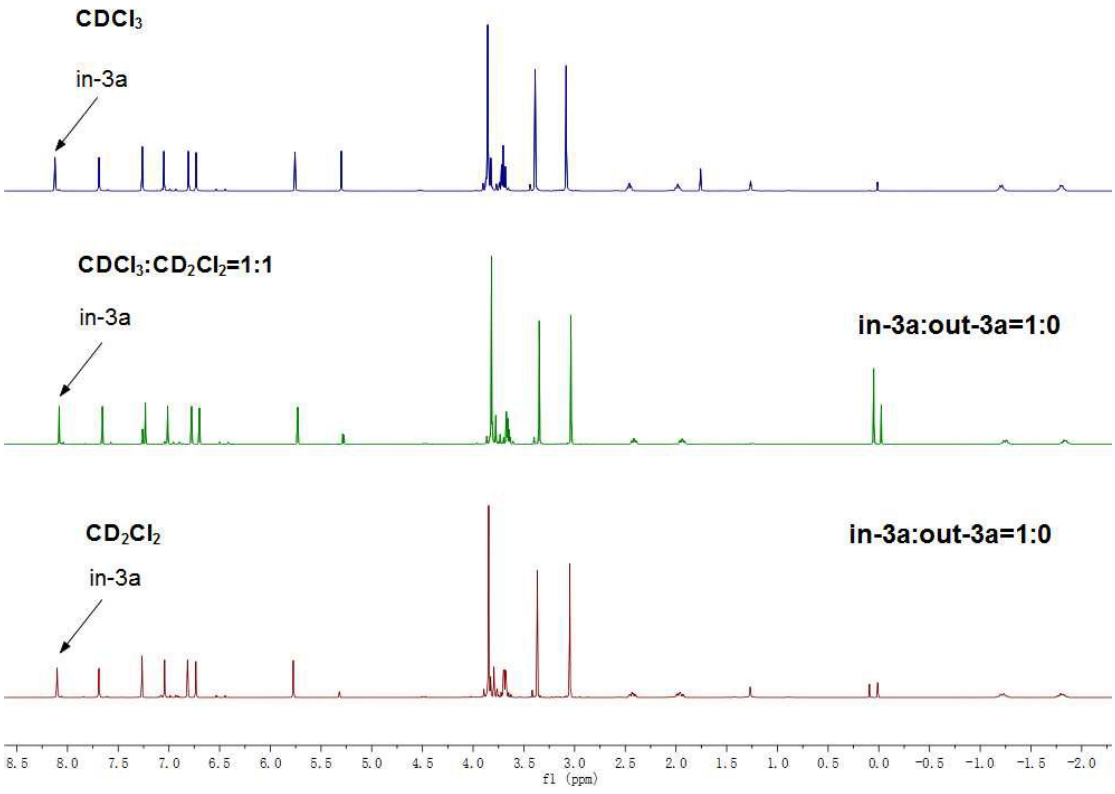

Fig. S26 ^{1}H NMR spectra (600 MHz) of compound **3a** in $CDCl_3$ (0.08 M) (top), $CDCl_3$-CD_2Cl_2 (1:1, v/v) (0.04 M)(middle), and CD_2Cl_2 (0.04 M) (bottom).

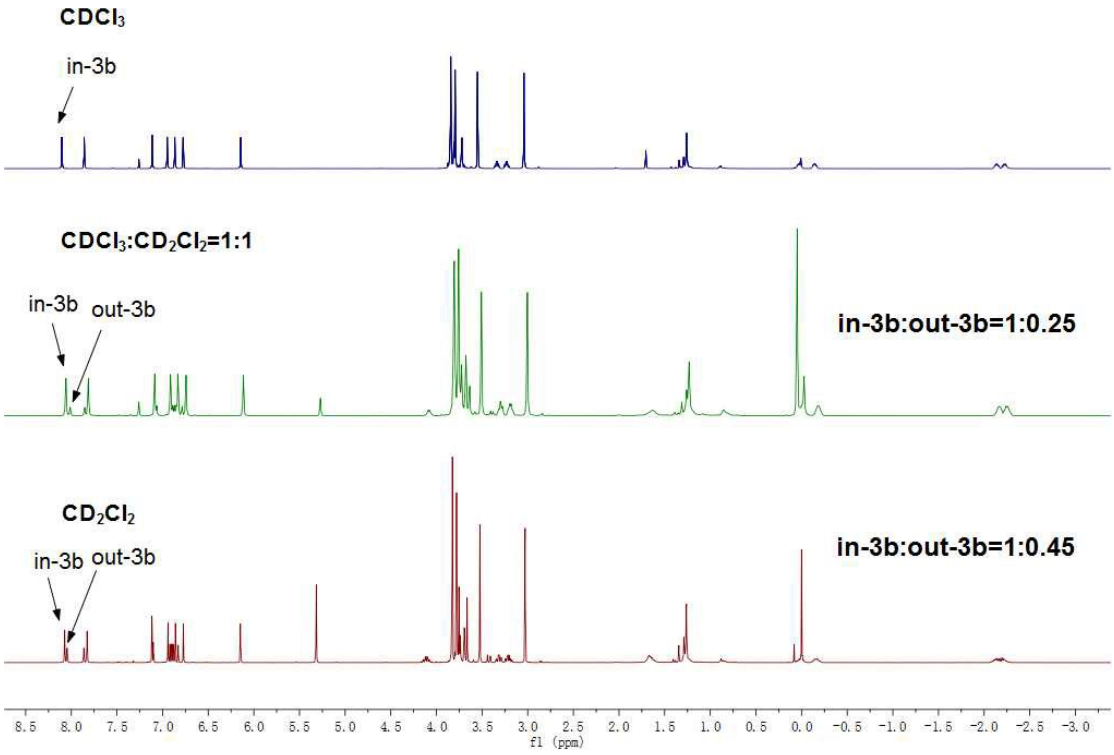

Fig. S27 ^{1}H NMR spectra (600 MHz) of compound **3b** in $CDCl_3$ (0.08 M) (top), $CDCl_3$-CD_2Cl_2 (1:1, v/v) (0.04 M)(middle), and CD_2Cl_2 (0.04 M) (bottom).

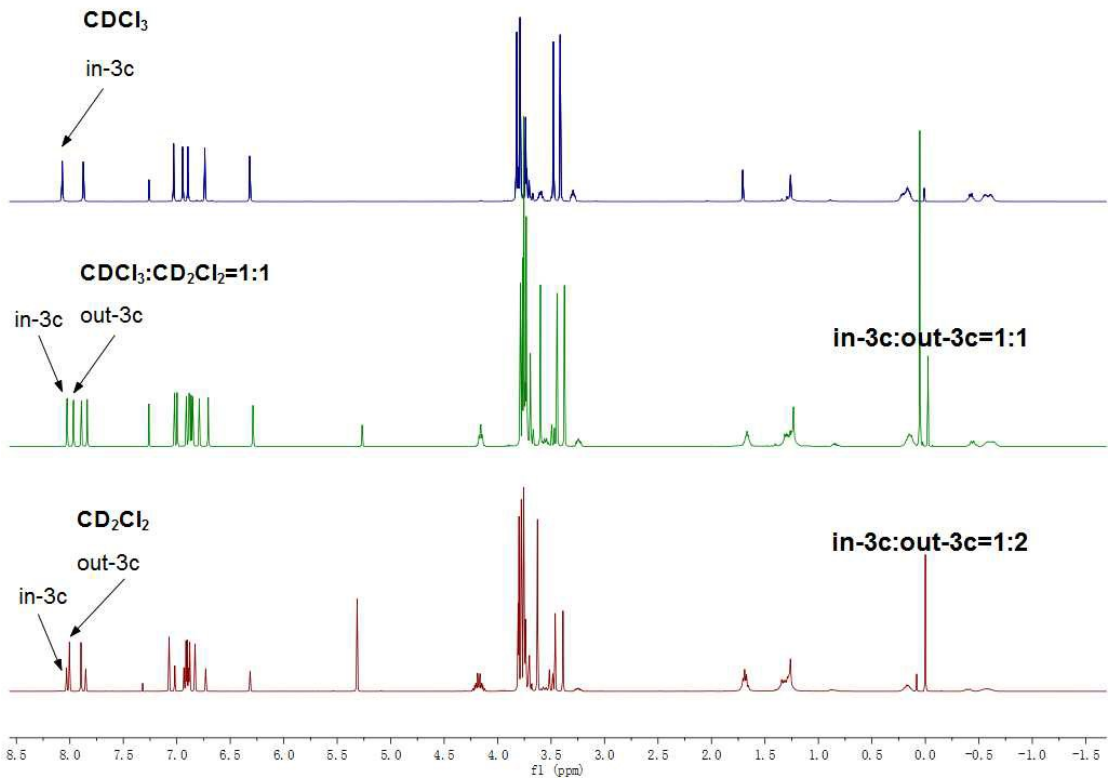

Fig. S28 ^{1}H NMR spectra (600 MHz) of compound **3c** in $CDCl_3$ (0.08 M) (top), $CDCl_3$-CD_2Cl_2 (1:1, v/v) (0.04 M)(middle), and CD_2Cl_2 (0.04 M) (bottom).

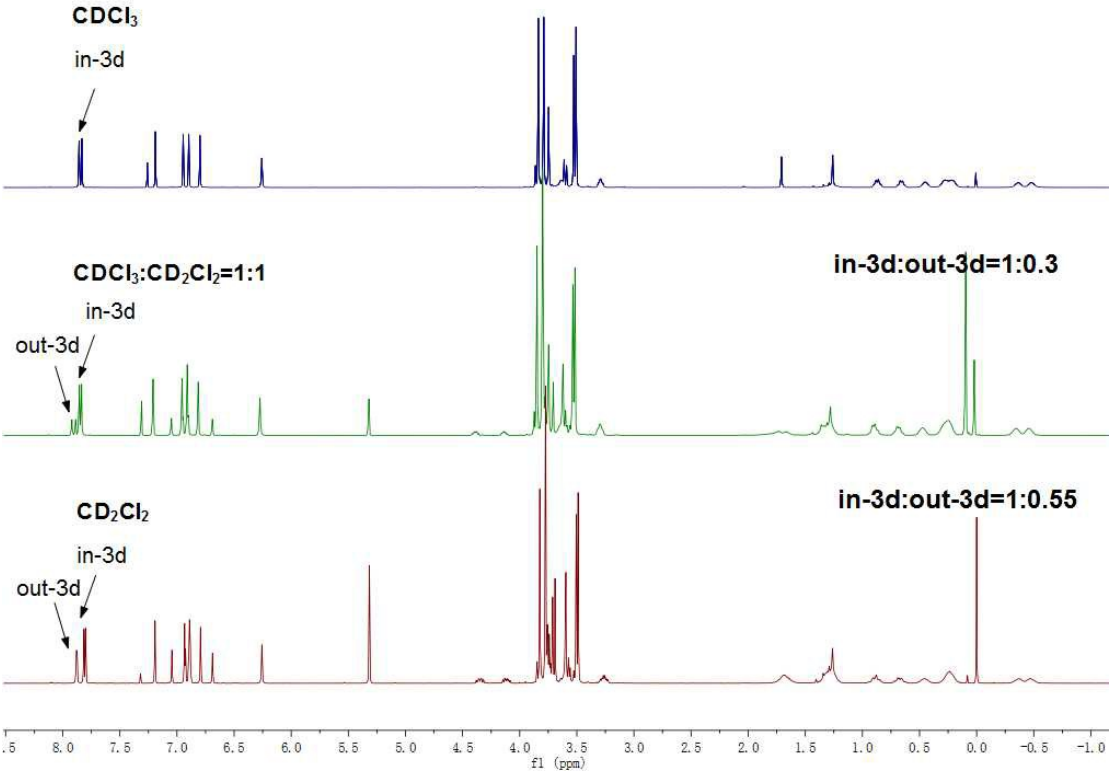

Fig. S29 ^{1}H NMR spectra (600 MHz) of compound **3d** in $CDCl_3$ (0.08 M) (top), $CDCl_3$-CD_2Cl_2 (1:1, v/v) (0.04 M)(middle), and CD_2Cl_2 (0.04 M) (bottom).

7. ^{1}H NMR Spectra for Host-Guest Complexation

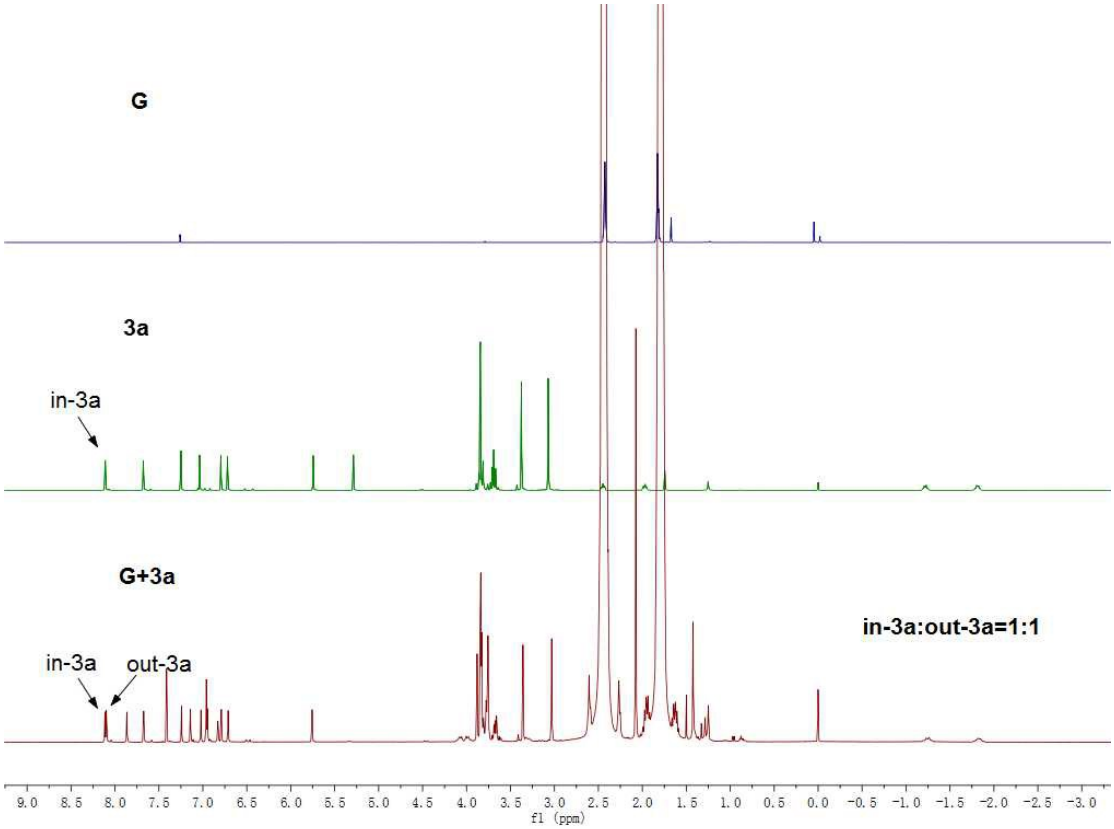

Fig. S30 ^{1}H NMR spectra (600 MHz, $CDCl_3$, 298 K) of **G** (0.01 M) (top), **3a** (0.04 M) (middle), and a mixture of **3a** with excess **G** (0.04M) (bottom).

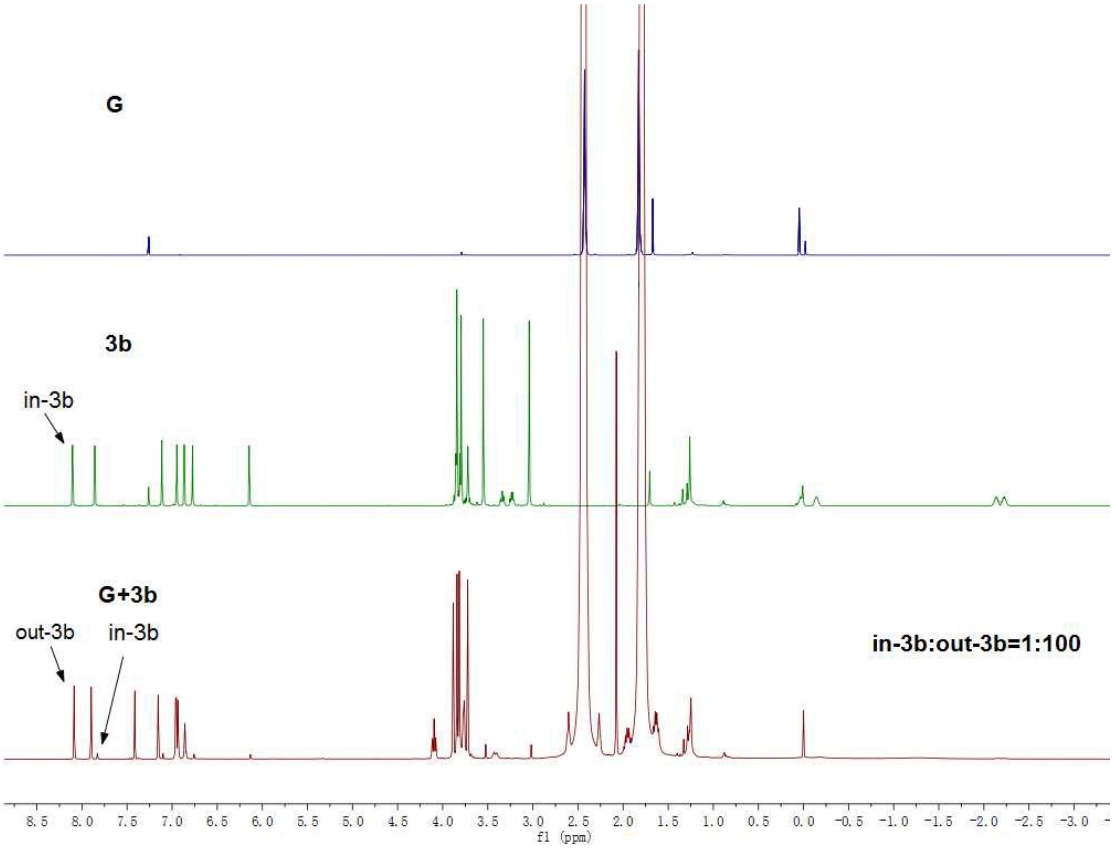

Fig. S31 ^{1}H NMR spectra (600 MHz, $CDCl_3$, 298 K) of **G** (0.01 M) (top), **3b** (0.04 M) (middle), and a mixture of **3b** with excess **G** (0.04M) (bottom).

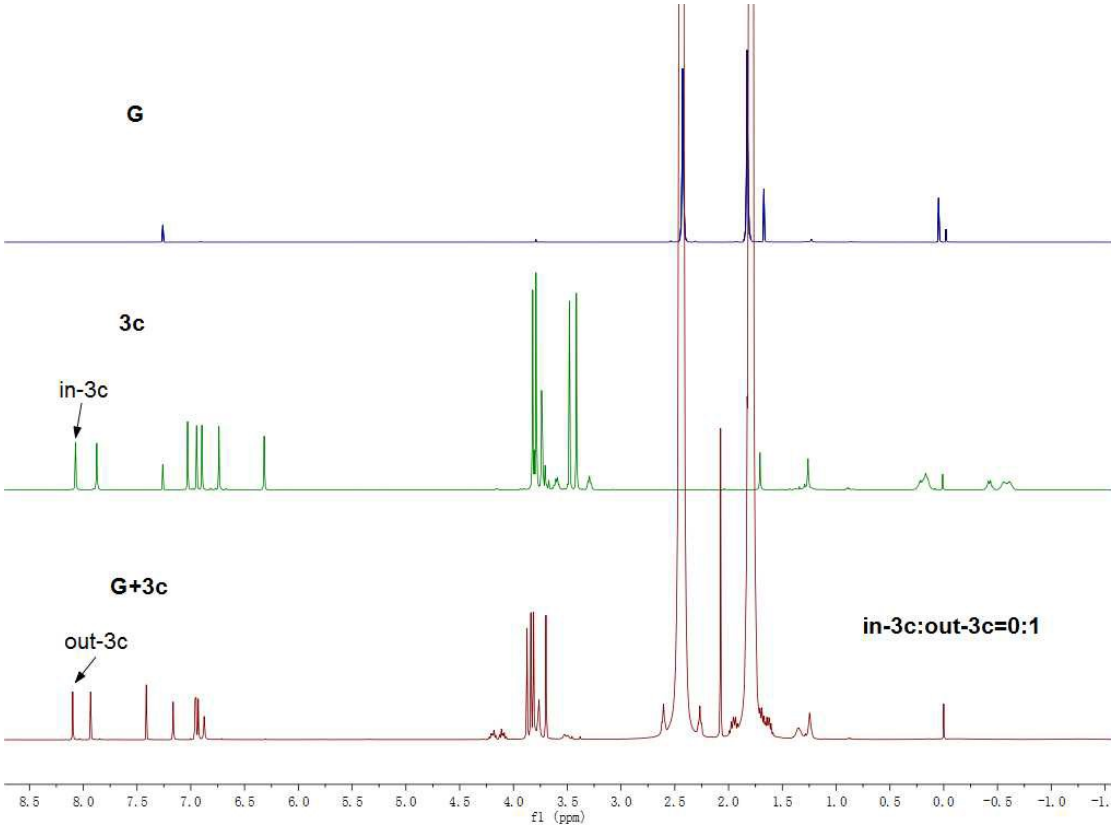

Fig. S32 ^{1}H NMR spectra (600 MHz, $CDCl_3$, 298 K) of **G** (0.01 M) (top), **3c** (0.04 M) (middle), and a mixture of **3c** with excess **G** (0.04M) (bottom).

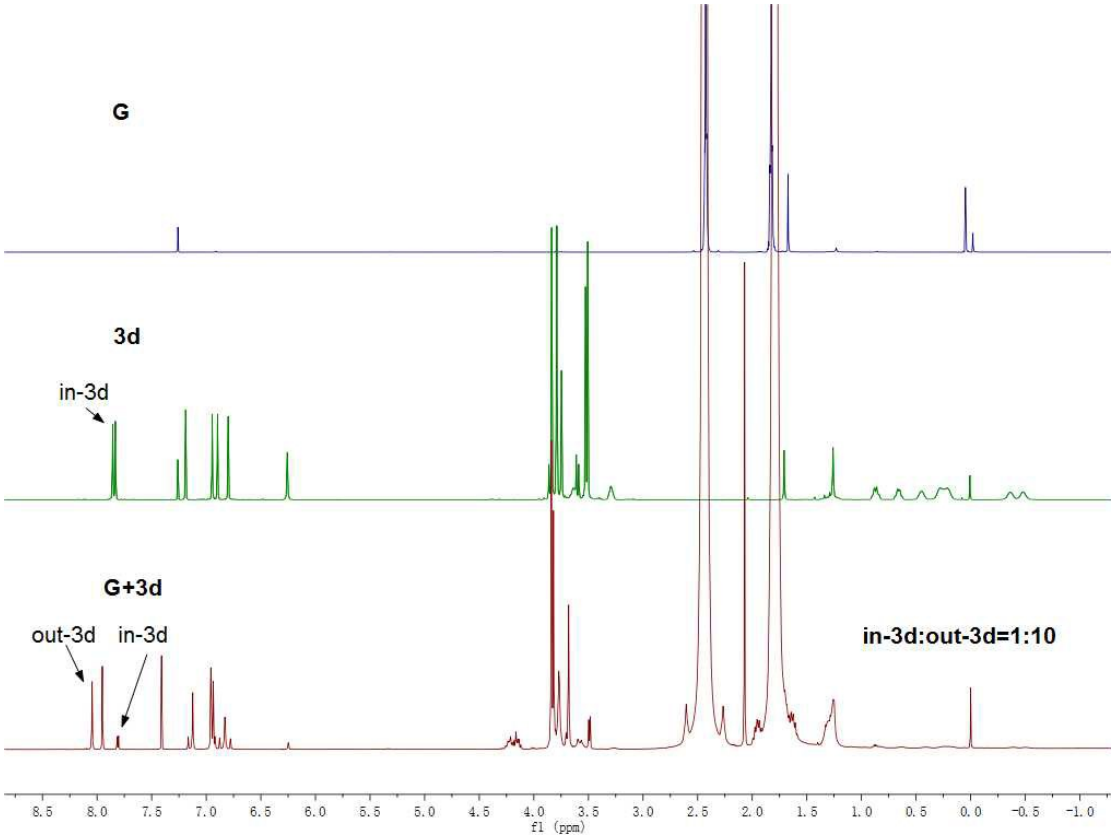

Fig. S33 ^{1}H NMR spectra (600 MHz, $CDCl_3$, 298 K) of **G** (0.01 M) (top), **3d** (0.04 M) (middle), and a mixture of **3d** with excess **G** (0.04M) (bottom).

8. Crystal structures of 3

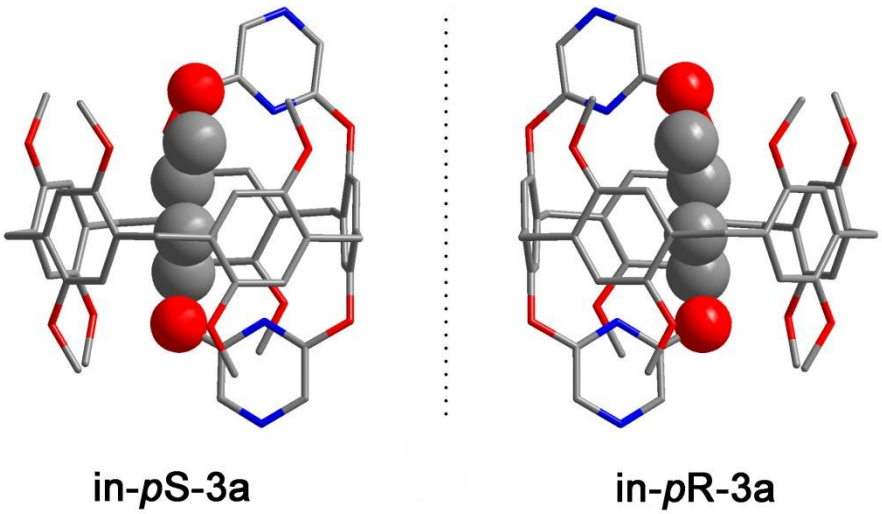

Fig. S34 Crystal structures of **3a.**

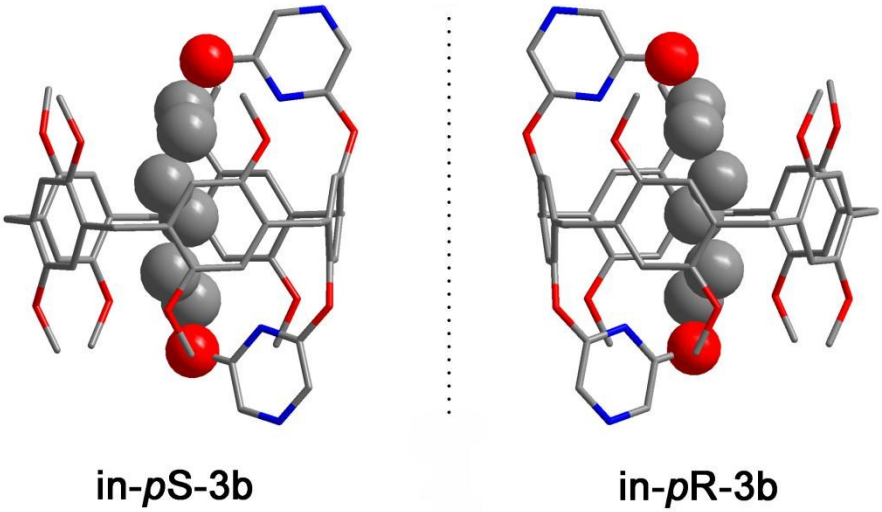

Fig. S35 Crystal structures of **3b.**

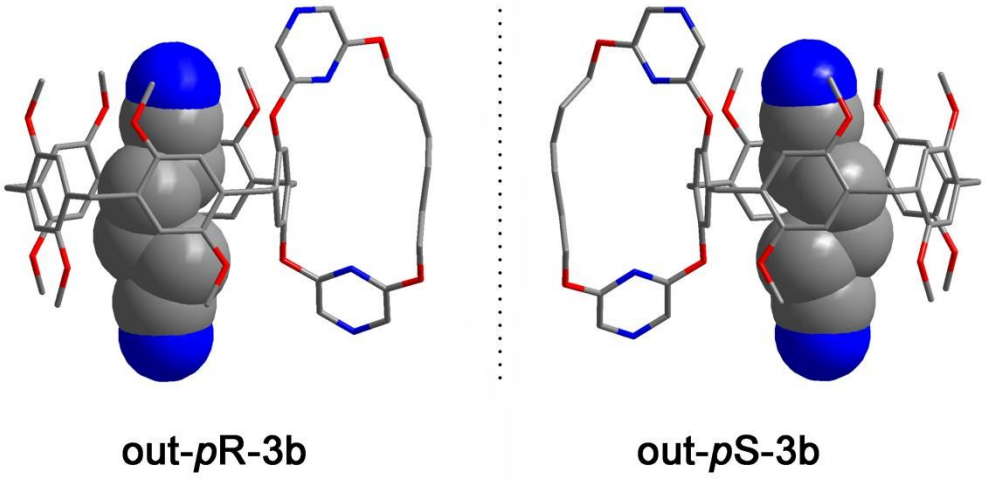

Fig. S36 Crystal structures of **G ⊂ 3b.**

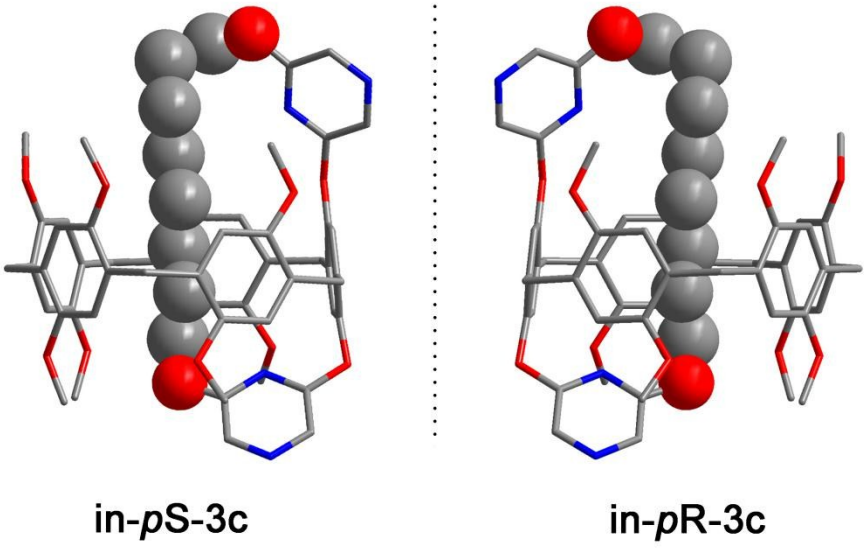

Fig. S37 Crystal structures of **3c.**

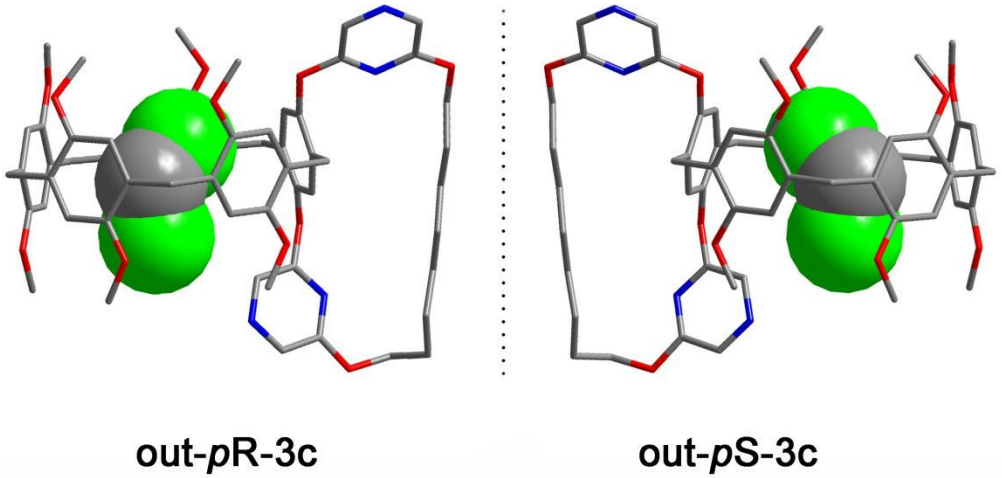

Fig. S38 Crystal structures of **DCM ⊂ 3c.**

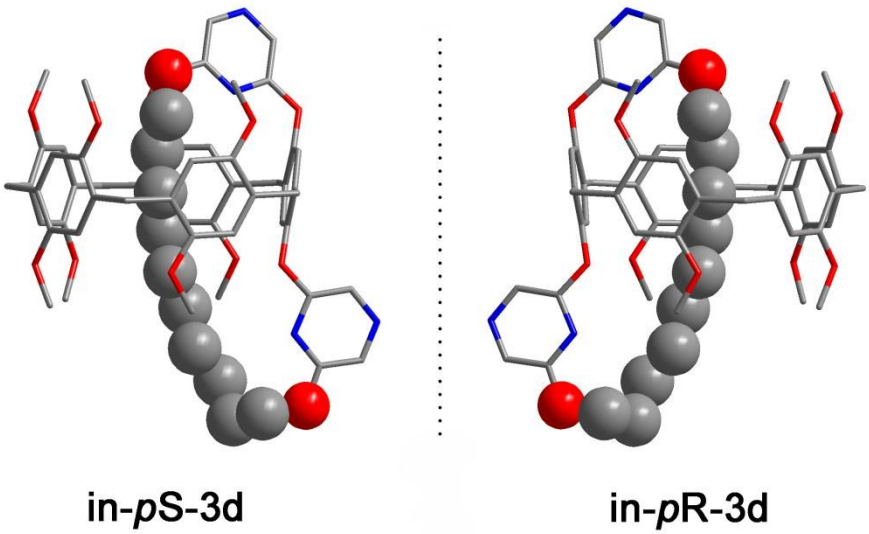

Fig. S39 Crystal structures of **3d.**

9. Chiral HPLC Trace of 3a and 3c

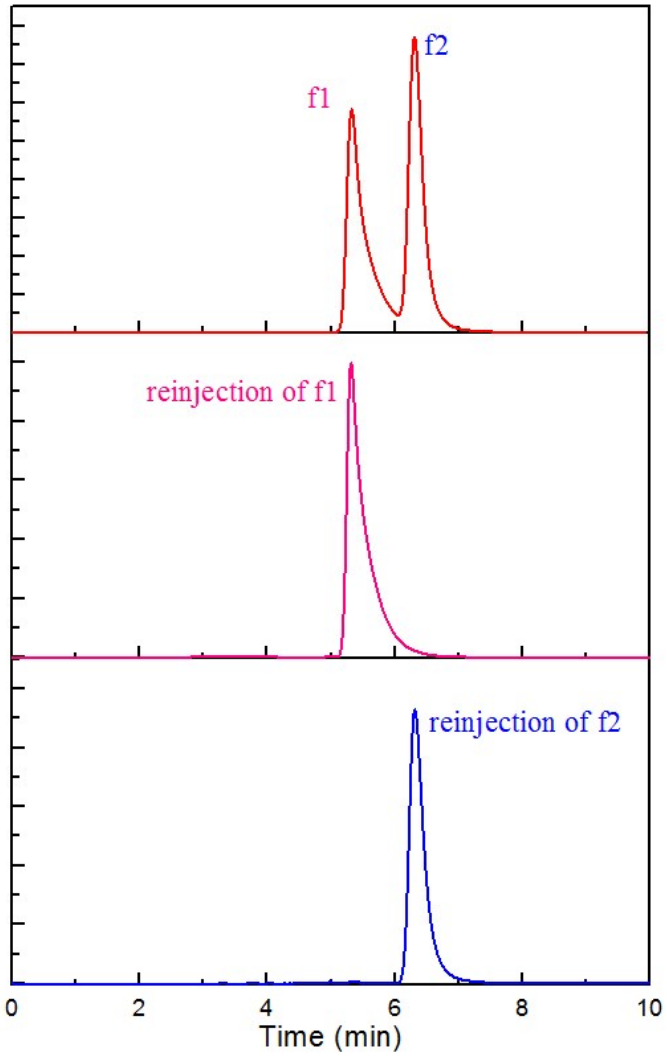

Fig. S40 Chiral-phase HPLC traces of **3a**, obtained by using a Chiralpak IA column eluted at 1 mL/min with 1:3 (v/v) THF/n-hexane (n-H), at 303 K.

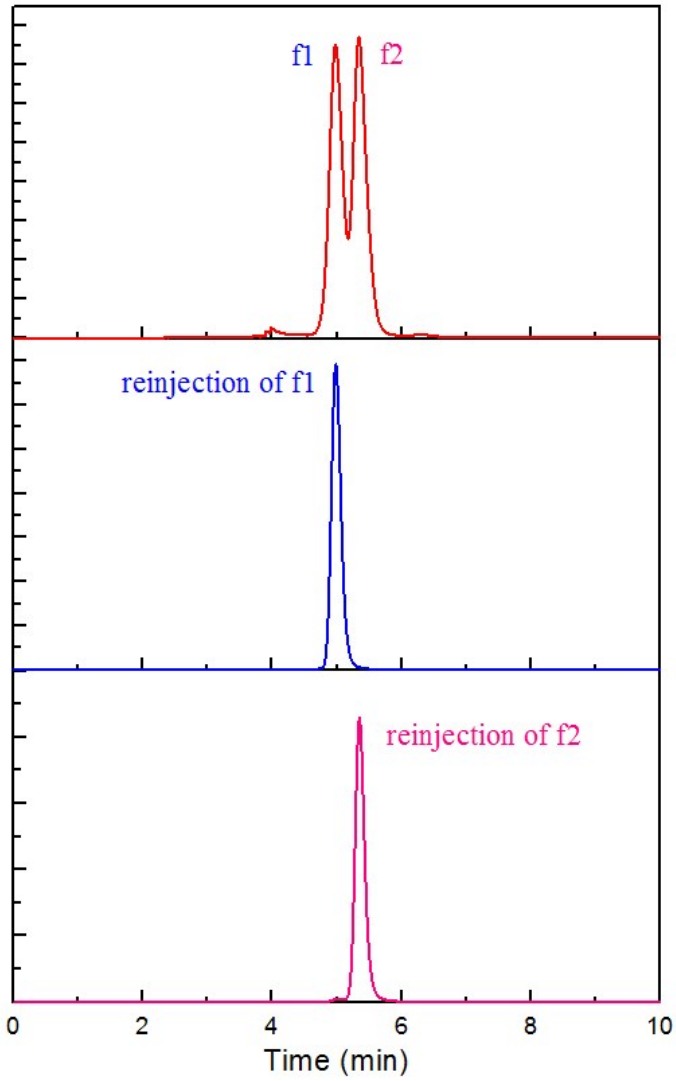

Fig. S41 Chiral-phase HPLC traces of **3c**, obtained by using a Chiralpak IA column eluted at 1 mL/min with 1:3 (v/v) THF/n-hexane (n-H), at 303 K.

10. Circular Dichroism (CD) Spectra and UV-vis spectra of 3a and 3c

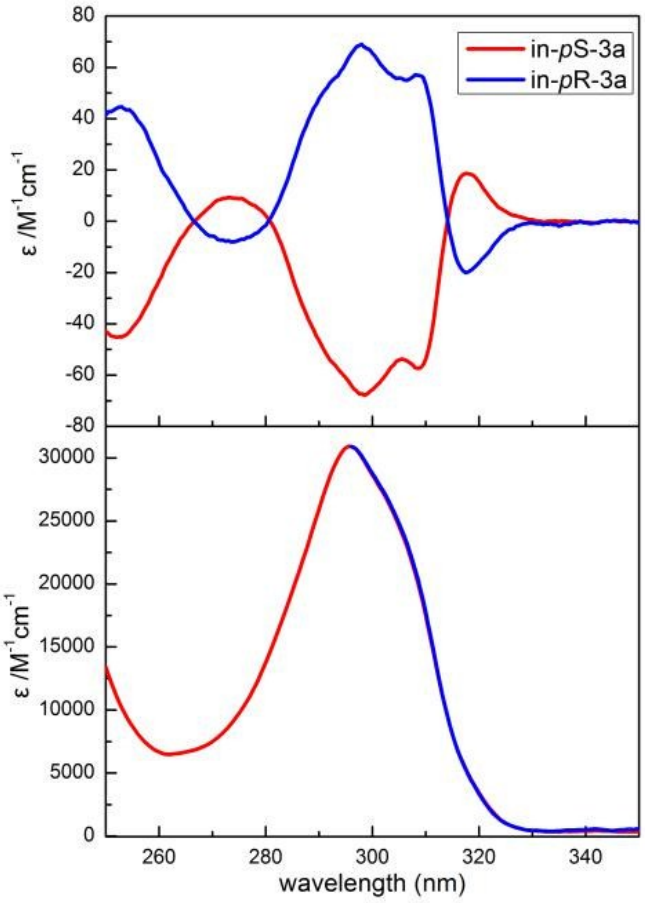

Fig. S42 Circular dichroism and UV-vis spectra (20 μM) **in-*p*S-3a** and **in-*p*R-3a** in $CHCl_3$ at 298 K.

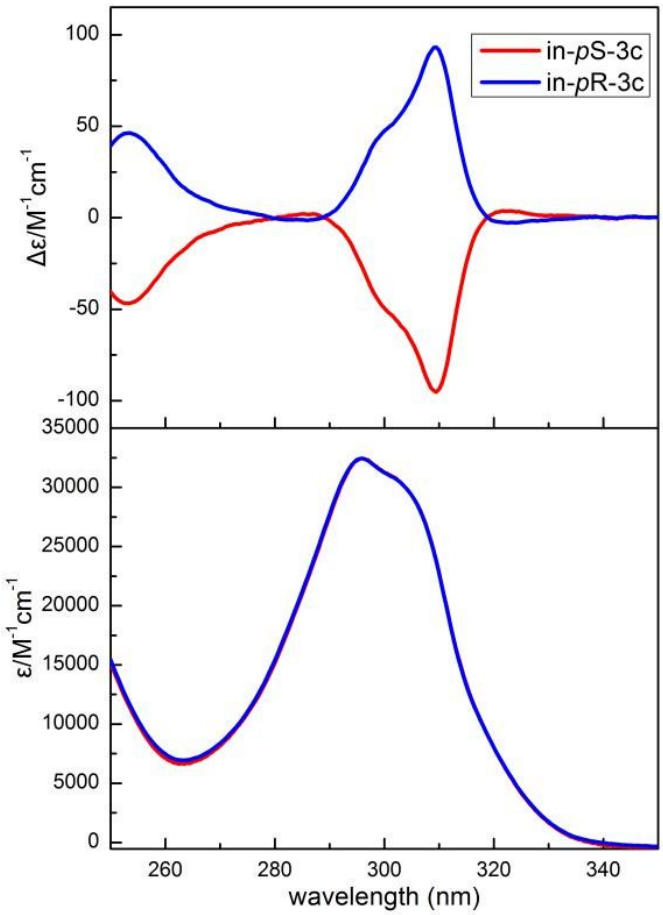

Fig. S43 Circular dichroism and UV-vis spectra (20 μM) **in-*p*S-3c** and **in-*p*R-3c** in $CHCl_3$ at 298 K.

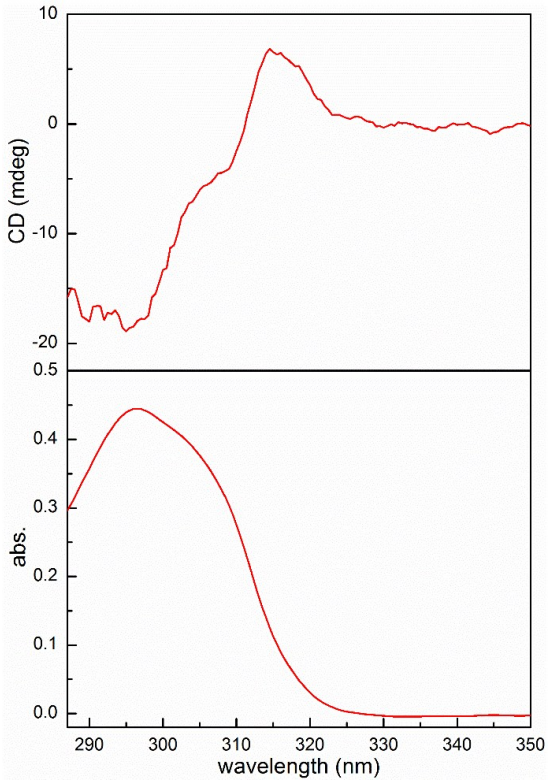

Fig. S44 Circular dichroism and UV-vis spectra (13.2 μM) **in-*p*S-3a** in adiponitrile at 298 K.

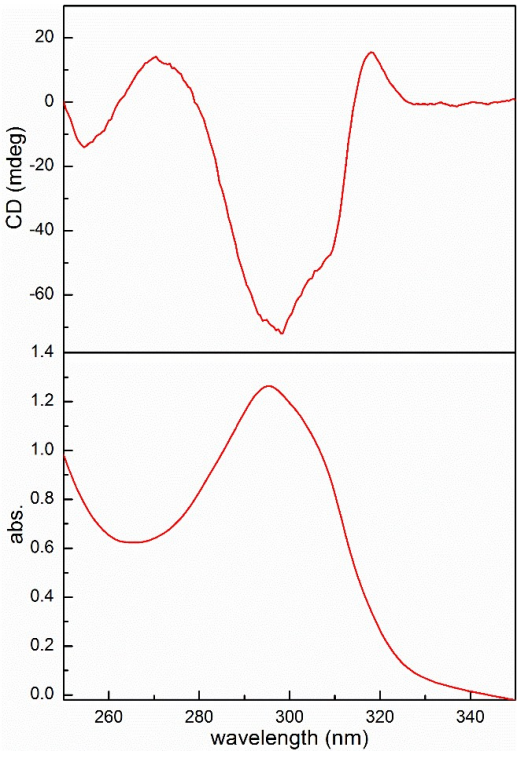

Fig. S45 Circular dichroism and UV-vis spectra of **in-*p*S-3a** in the solid state at 298 K.

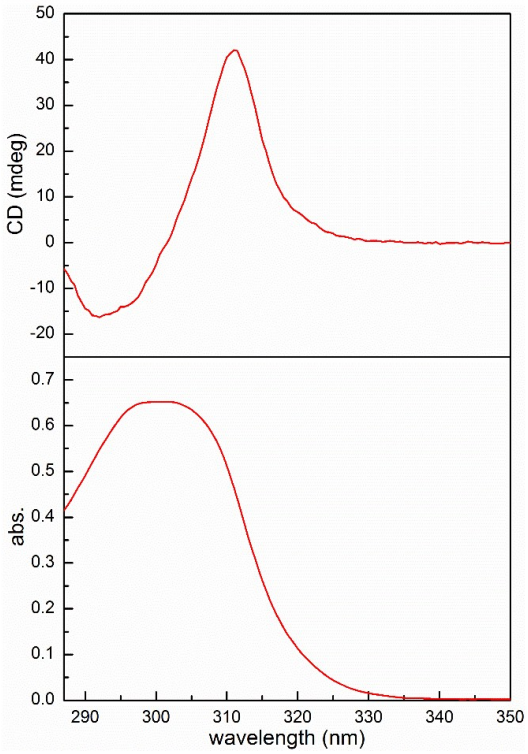

Fig. S46 Circular dichroism and UV-vis spectra (15.7 μM) of **in-*p*S-3c** in adiponitrile at 298 K.

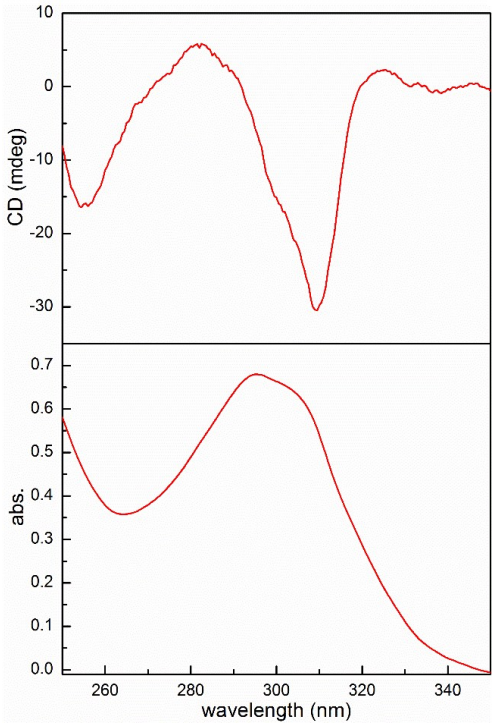

Fig. S47 Circular dichroism and UV-vis spectra of **in-*p*S-3c** in the solid state at 298 K.

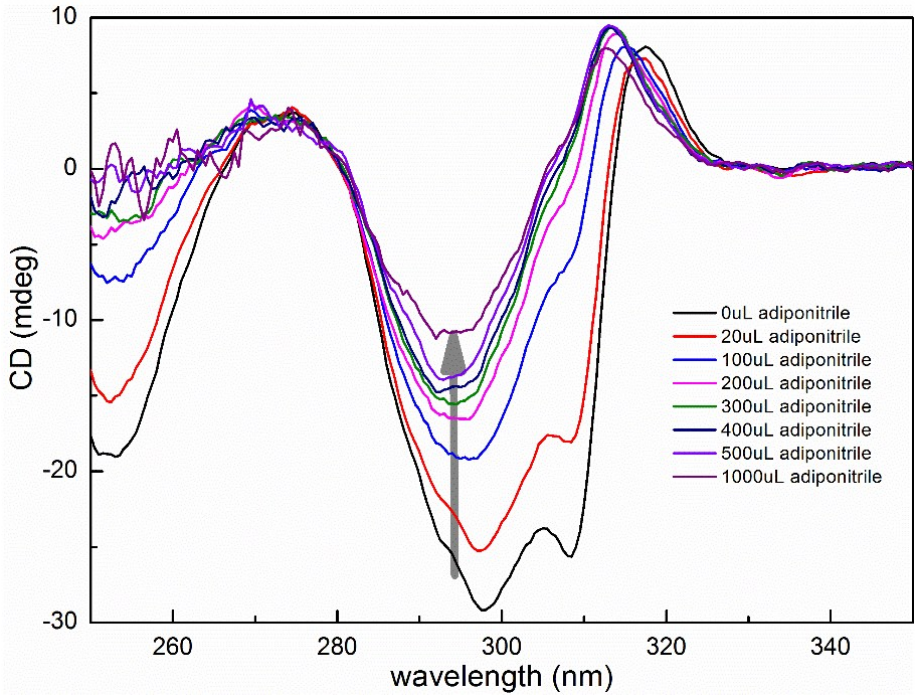

Fig. S48 CD spectra (13.2μM, 2mL $CHCl_3$, room temperature, black line) of **in-*p*S-3a** and its spectral changes upon addition of adiponitrile (0–1000 μL).

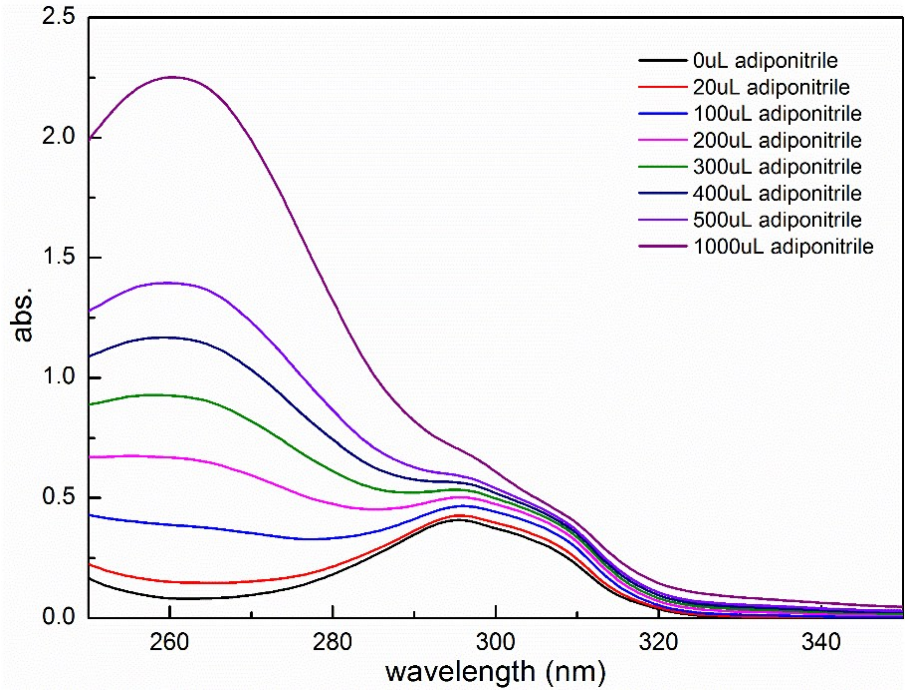

Fig. S49 UV-vis spectra (13.2μM, 2mL $CHCl_3$, room temperature, black line) of **in-*p*S-3a** and its spectral changes upon addition of adiponitrile (0–1000 μL).

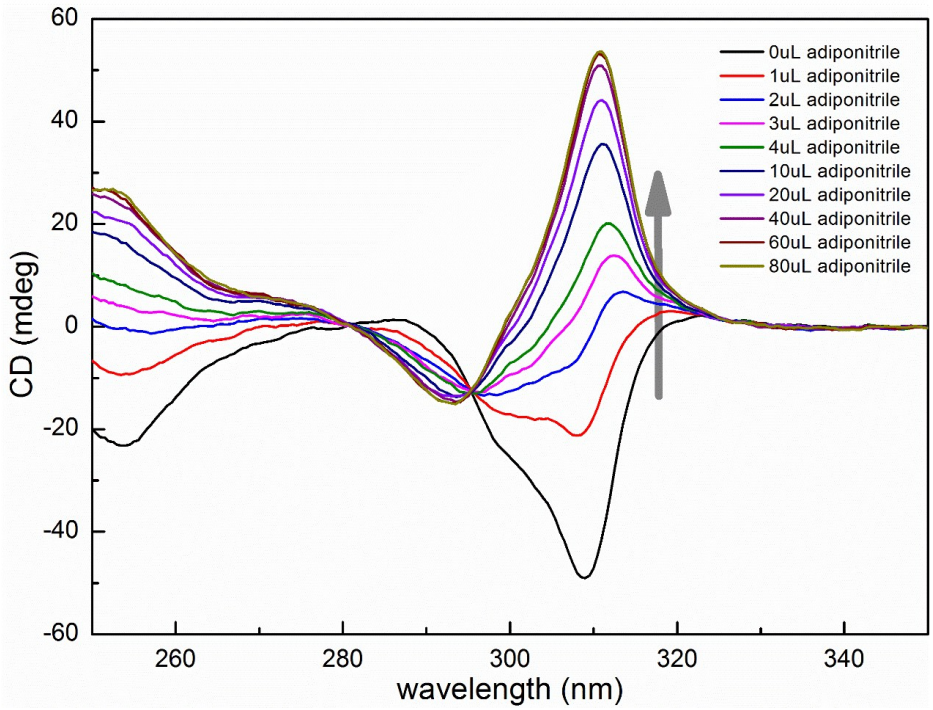

Fig. S50 CD spectra (15.7μM, 2mL $CHCl_3$, room temperature, black line) of **in-*p*S-3c** and its spectral changes upon addition of adiponitrile (0–80 μL).

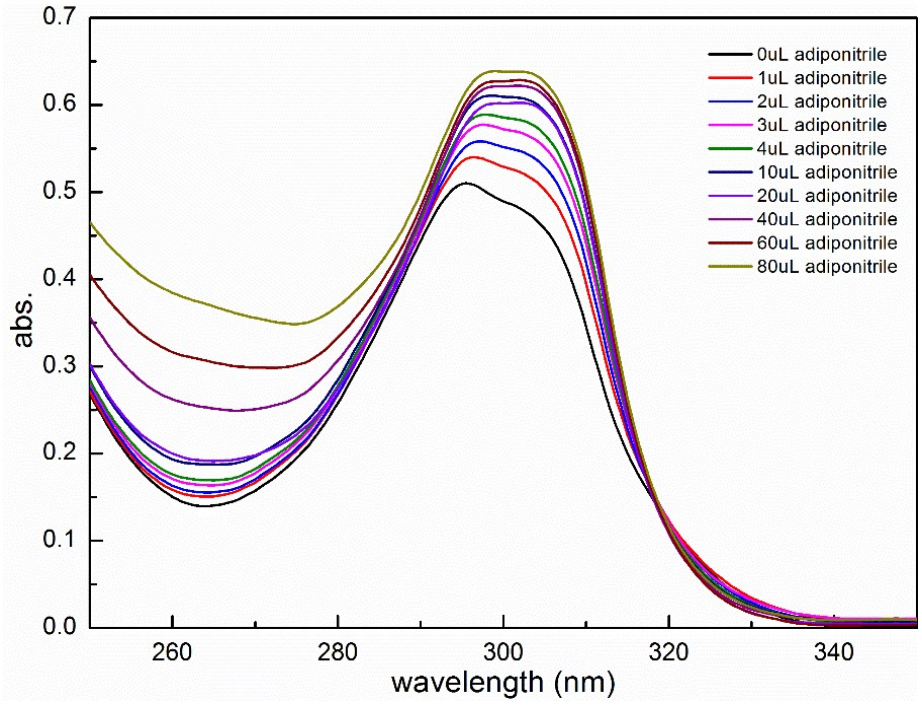

Fig. S51 UV-vis spectra (15.7μM, 2mL $CHCl_3$, room temperature, black line) of **in-*p*S-3c** and its spectral changes upon addition of adiponitrile (0–80 μL).

11. DFT Calculated CD Spectra of 3a and 3c

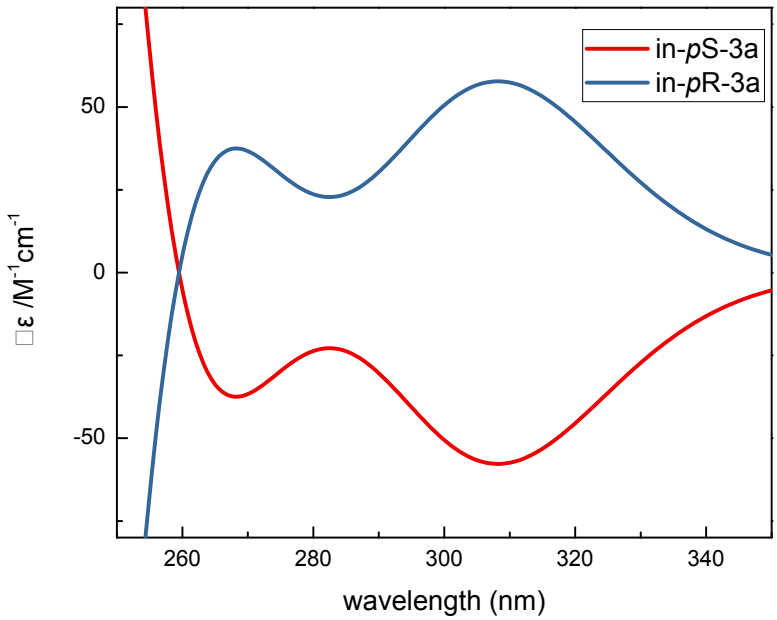

Fig. S52 Calculated CD spectra of in-*p*S-**3a** and in-*p*R-**3a** at the CAM-B3LYP/DGTZVP level. Wavelengths were 30nm red-shifted.

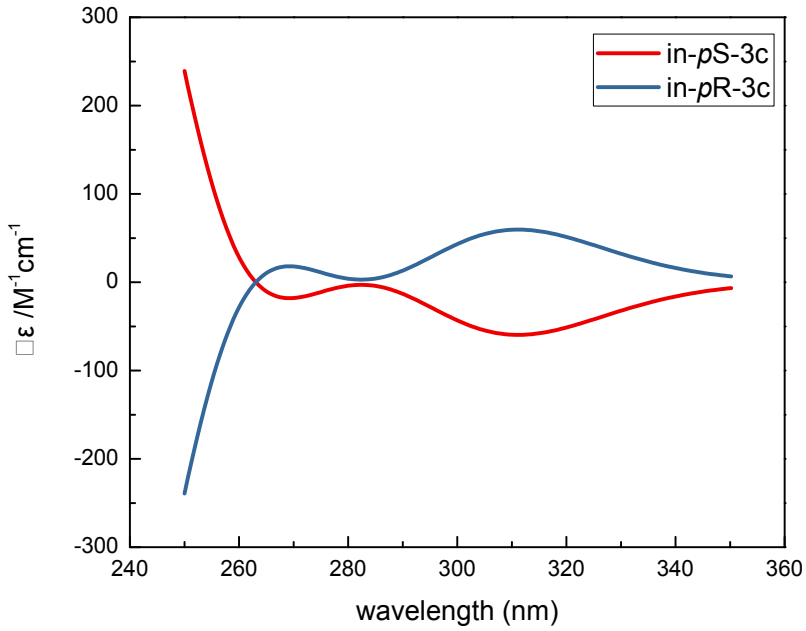

Fig. S53 Calculated CD spectra of in-*p*S-**3c** and in-*p*R-**3c** at the CAM-B3LYP/DGTZVP level. Wavelengths were 30nm red-shifted.

12. DFT Calculation of Relative Energy Differences

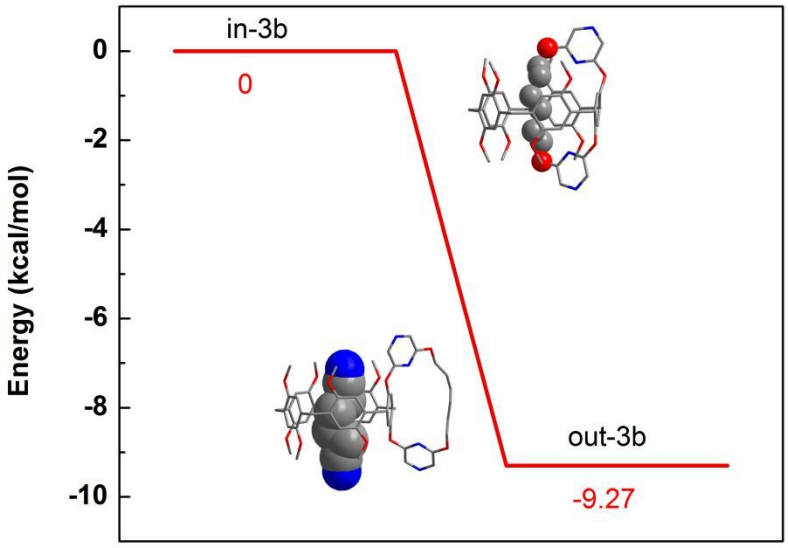

Fig. S54 Calculated relative energy of in-**3b** and out-**3b** in $CHCl_3$.

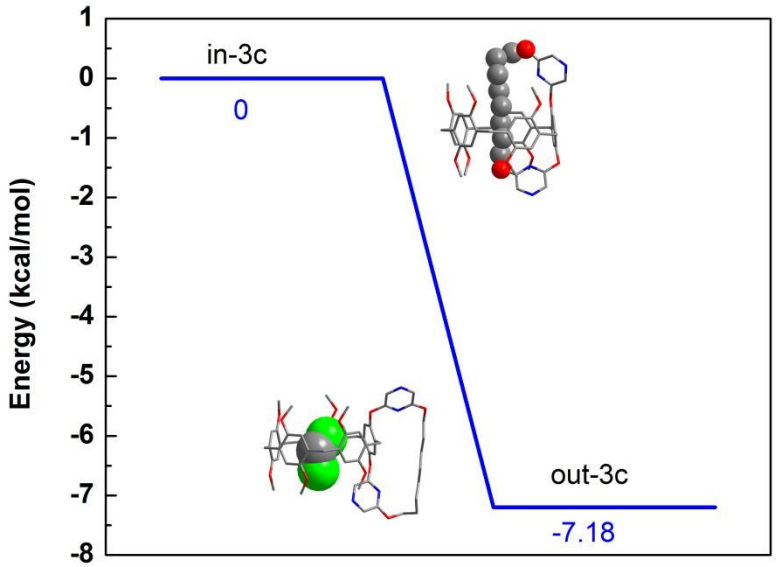

Fig. S55 Calculated relative energy of in-**3c** and out-**3c** in CH_2Cl_2.

13. References

1. A. D. Becke, *J. Chem. Phys.* 1993, **98**, 5648-5652.

2. C. Sosa, J. Andzelm, B. C. Elkin, E. Wimmer, K. D. Dobbs, D. A. Dixon, *J. Phys. Chem.*, 1992, **96**, 6630-36.

3. J. Tomasi, B. Mennucci, and R. Cammi, *Chem. Rev.*, 2005, **105**, 2999-3093.

4. M. J. Frisch, G. W. Trucks, H. B. Schlegel, G. E. Scuseria, M. A. Robb, J. R. Cheeseman, G. Scalmani, V. Barone, B. Mennucci,G. A. Petersson, Gaussian, Inc, Wallingford CT, 2009.